AD-A056 322 AVCO SYSTEMS DIV WILMINGTON MASS F/G 19/4
IMPACT AND PENETRATION TECHNOLOGY PROGRAM SHOCK ATTENUATION TES--ETC(U)
AUG 77 E J GIARA, P J GRADY DNA001-75-C-0181
UNCLASSIFIED AVSD-0242-77-CR DNA-4414F NL

1 OF 1
ADA
056322

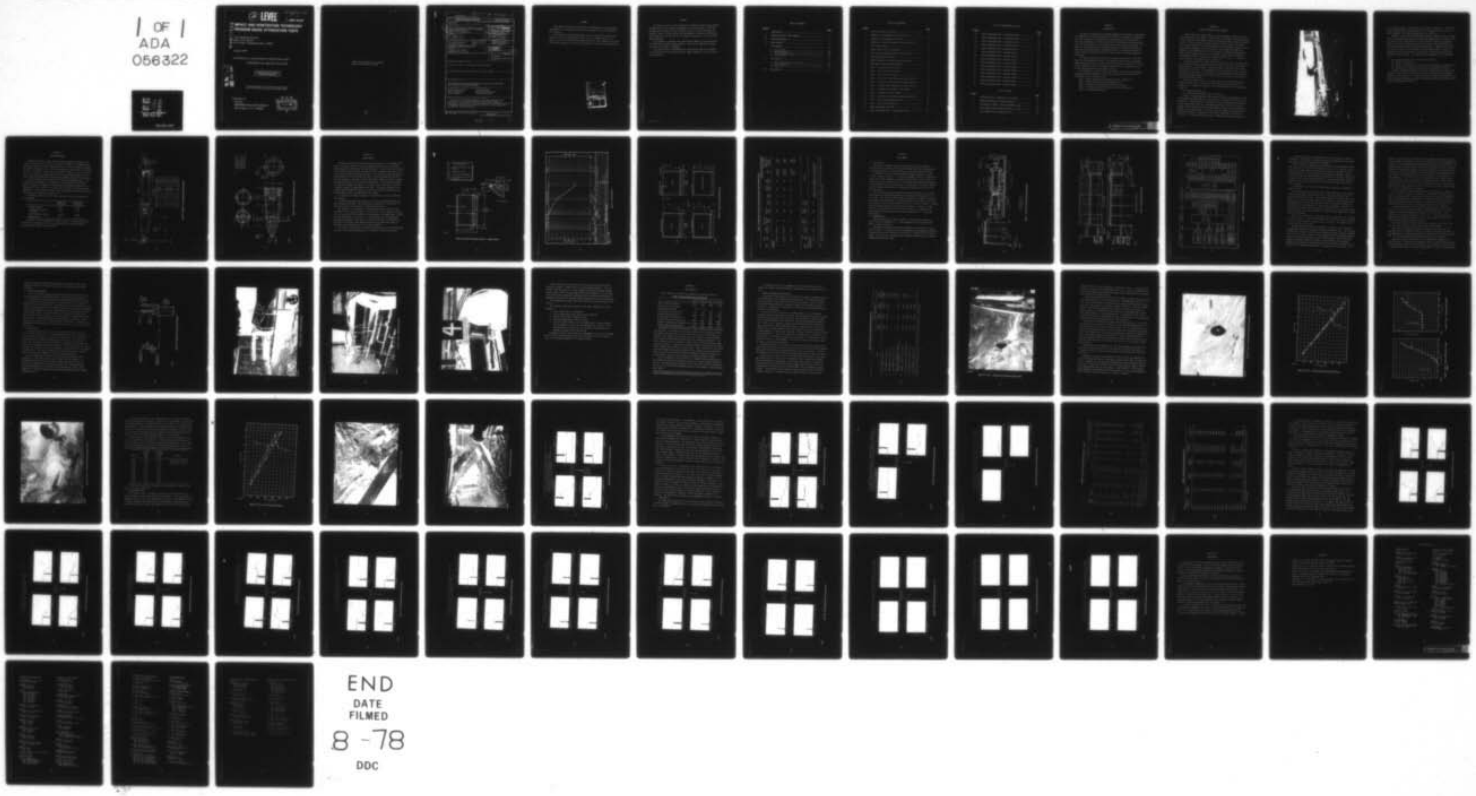

END
DATE
FILMED
8-78
DDC

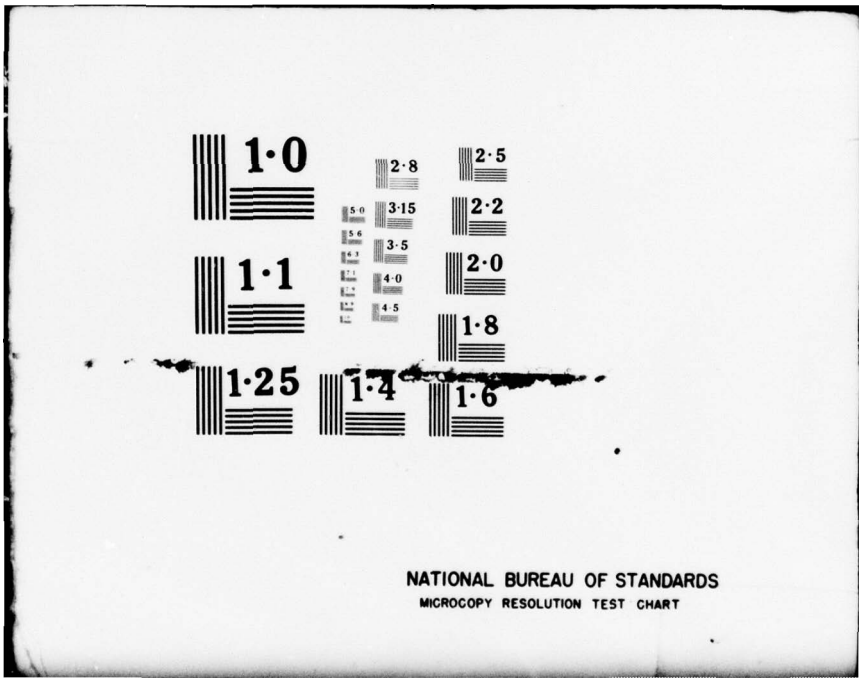
1·0
1·1
1·25
1·4
1·6
1·8
2·0
2·2
2·5
2·8
3·15
3·5
4·0
4·5
5·0
5·6
NATIONAL BUREAU OF STANDARDS
MICROCOPY RESOLUTION TEST CHART

(12) LEVEL II

DNA 4414F

IMPACT AND PENETRATION TECHNOLOGY PROGRAM SHOCK ATTENUATION TESTS

Avco Systems Division
201 Lowell Street
Wilmington, Massachusetts 01887

August 1977

Final Report for Period 20 April 1976—31 May 1977

CONTRACT No. DNA 001-75-C-0181

APPROVED FOR PUBLIC RELEASE;
DISTRIBUTION UNLIMITED.

THIS WORK SPONSORED BY THE DEFENSE NUCLEAR AGENCY
UNDER RDT&E RMSS CODE B344075464 Y99QAXSB04807 H2590D.

Prepared for
Director
DEFENSE NUCLEAR AGENCY
Washington, D. C. 20305

Destroy this report when it is no longer needed. Do not return to sender.

(18) DNA (SBIE) (19) 4414F, AD-E300 236

UNCLASSIFIED

SECURITY CLASSIFICATION OF THIS PAGE *(When Data Entered)*

REPORT DOCUMENTATION PAGE

READ INSTRUCTIONS BEFORE COMPLETING FORM

1. REPORT NUMBER: DNA 4414F
2. GOVT ACCESSION NO.
3. RECIPIENT'S CATALOG NUMBER

4. TITLE *(and Subtitle)*: IMPACT AND PENETRATION TECHNOLOGY PROGRAM SHOCK ATTENUATION TESTS.

5. TYPE OF REPORT & PERIOD COVERED: Final Report for Period 20 Apr 76—31 May 77

6. PERFORMING ORG. REPORT NUMBER: AVSD-0242-77-CR

7. AUTHOR(s): E. J. Giara, Jr.
P. J. Grady, Jr

8. CONTRACT OR GRANT NUMBER(s): DNA 001-75-C-0181

9. PERFORMING ORGANIZATION NAME AND ADDRESS:
Avco Systems Division
201 Lowell Street
Wilmington, Massachusetts 01887

10. PROGRAM ELEMENT, PROJECT, TASK AREA & WORK UNIT NUMBERS: Subtask Y99QAXSB048-07

11. CONTROLLING OFFICE NAME AND ADDRESS:
Director
Defense Nuclear Agency
Washington, D.C. 20305

12. REPORT DATE: August 1977

13. NUMBER OF PAGES: 72

14. MONITORING AGENCY NAME & ADDRESS *(if different from Controlling Office)*

15. SECURITY CLASS *(of this report)*: UNCLASSIFIED

15a. DECLASSIFICATION/DOWNGRADING SCHEDULE

16. DISTRIBUTION STATEMENT *(of this Report)*

Approved for public release; distribution unlimited.

17. DISTRIBUTION STATEMENT *(of the abstract entered in Block 20, if different from Report)*

18. SUPPLEMENTARY NOTES

This work sponsored by the Defense Nuclear Agency under RDT&E RMSS Code B344075464 Y99QAXSB04807 H2590D.

19. KEY WORDS *(Continue on reverse side if necessary and identify by block number)*

Reverse Ballistic Test	Off-Normal Impact
Impact Strain Data	Impact Acceleration Data
Earth Penetrator	High Velocity Impact

20. ABSTRACT *(Continue on reverse side if necessary and identify by block number)*

A series of four reverse ballistics tests were performed on two different types of earth penetrators at various impact angles and obliquities. The objective of this test series was to provide an improved and expanded strain and acceleration data base for critical impact environments on earth penetrators.

DD FORM 1 JAN 73 1473 EDITION OF 1 NOV 65 IS OBSOLETE

UNCLASSIFIED

SECURITY CLASSIFICATION OF THIS PAGE *(When Data Entered)*

404 788

SUMMARY

This report describes the fabrication, instrumentation, test procedures and results of four reverse ballistics tests conducted at the Avco Ballistic Test Facility.

The testing was performed using the Avco 15.2-inch gun to propel media targets of concrete and compressed sandy till at a nominal velocity of 1500 ft/s into two different earth penetrators (EP). The resultant strain and acceleration response of the EP's were recorded at several critical locations.

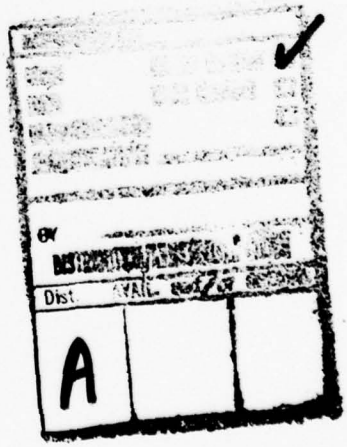

PREFACE

The objective of this test series was to provide an improved and expanded data base for critical impact environments on earth penetrators. This was accomplished by reverse ballistic testing a total of four instrumented projectiles, three at various obliquities and angles of attack on the DNA half-scale penetrator, and one test at a 5^{o} angle of attack on a 1/8 scale low L/D model penetrator.

The program was conducted under Modification P00002 to Contract DNA 001-75-C-0181 for the Defense Nuclear Agency. The work was administered under the direction of Major D. Spangler.

The author wishes to acknowledge the contributions made by the members of the Avco Ballistics Laboratory and Mr. Edward Plamowski of the Avco Structures Laboratory.

TABLE OF CONTENTS

LIST OF ILLUSTRATIONS

LIST OF ILLUSTRATIONS (Concl'd)

LIST OF TABLES

SECTION I

INTRODUCTION

The Impact and Penetration Technology Program was initiated to demonstrate the capability of analytical techniques to predict the response of representative earth penetrator configurations following impact with various media. This was accomplished by careful selection of configuration and impact parameters that would exercise a particular effect on the projectile response. In addition, a detailed study of the required types of instrumentation and the manner in which electronically obtained data were recorded was necessary to obtain reliable experimental data that could be used to evaluate analytical predictions.

This report details the results of the final task (Task 6) of this program, the Shock Attenuation Tests. The purpose of this task is to provide additional response data for correlation with analytical predictors. The test series consisted of four tests with both high and low L/D penetrators with various impact obliquities and angles of attack.

The chronology of earlier Avco studies under the Impact and Penetration Technology Program (DNA 001-C-75-0181) over the period from February 1975 through May 1977 is described below.

Task 1 Impact and Penetration Parametric Study (Reference 1)

Task 2 Reverse Ballistic Testing (Reference 2)

Task 3 Materials Investigations and Model Generation

Task 4 P-2 Half Scale Reverse Ballistic Testing (Reference 4)

Task 5 Off-normal Impact Study

SECTION II

REVERSE BALLISTIC TEST TECHNIQUE

Reverse ballistic testing (RBT), as the name implies, involves ballistic tests during which the target is impacted into a stationary projectile instead of the projectile being impacted into the stationary target. Reverse ballistic testing is used in place of standard ballistic tests to reduce the overall cost, and to improve the quality and quantity of data gathered from each test. The principal advantage of this procedure is that significant numbers of channels of instrumentation can be "hard lined" to standard recording equipment, thereby eliminating the need for channel-limited high "g" telemetry systems which would be required for straight ballistic shots. A typical reverse ballistic test setup is shown in Figure 1.

The forces experienced during an RBT are the same as would be experienced in a projectile during a standard ballistic test, if the size of the target being impacted is large enough to preclude boundary wave reflections in the time window of interest. The equivalence of the two types of tests is demonstrated by the fact that in a coordinate system transformation which involves translational displacement and/or velocity alone, the forces are invariant in a Galilean reference frame.

One of the areas in which a variation from the standard ballistic test results would be found is caused by the practical aspect associated with having to use a limited size target. This limitation results in discrepancies caused by:

- momentum exchange, and
- stress wave reflections from free surfaces.

During a straight ballistic impact event the projectile undergoes a rigid body deceleration dependent only on the interaction forces and the mass of the projectile. During an RBT this deceleration is also dependent on the inertia of the target media which for a reasonable simulation, the initial kinetic energy of the target media would be much greater than the work done during the duration of the impact event. In other words, the target media should be as massive as possible to simulate the real event by adapting a semi-infinite half space. A large mass directly affects target media velocity change, i.e.,

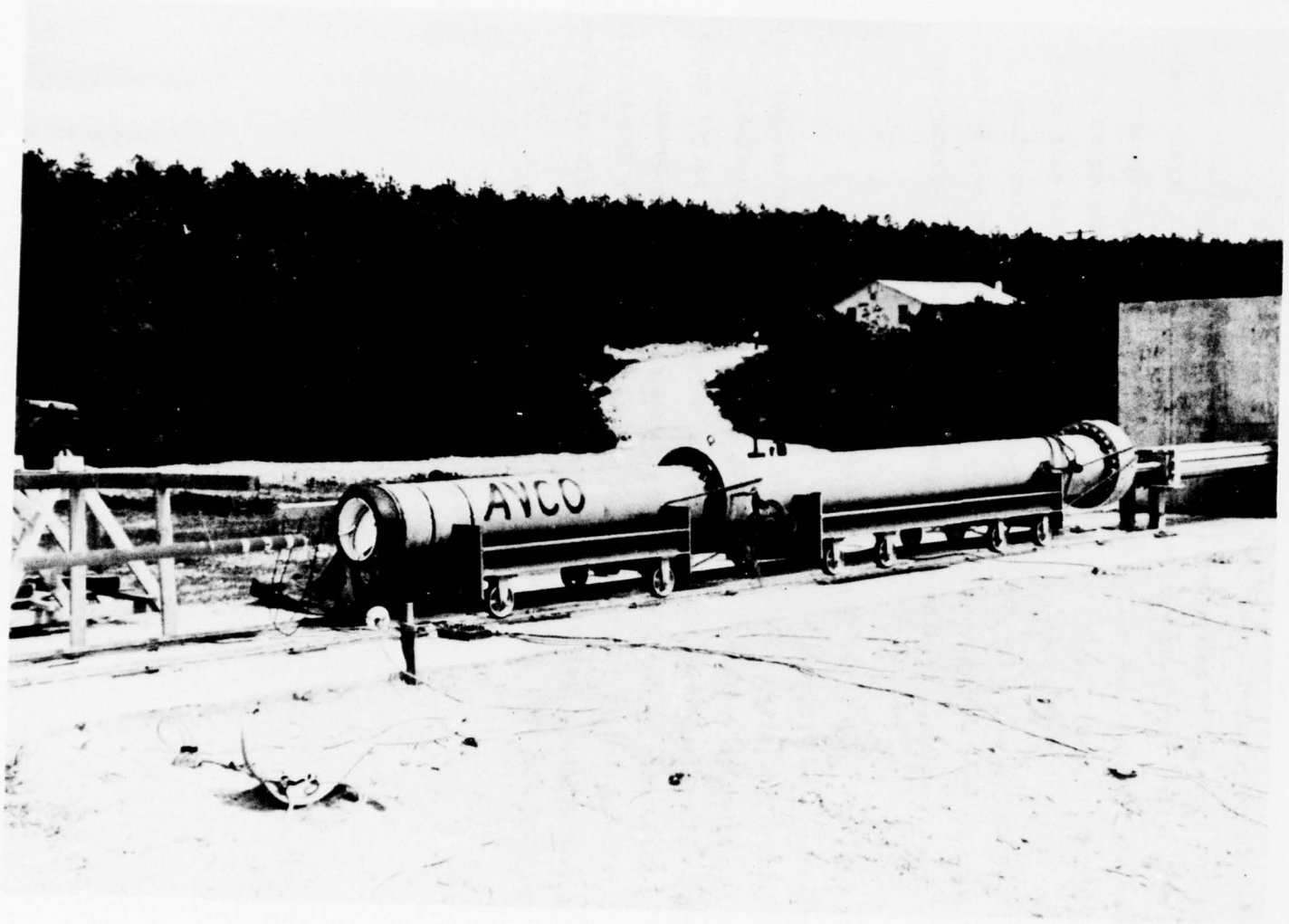

23913-C

Figure 1. Reverse ballistic test setup.

a low velocity change is an indicator of a realistic simulation. In the tests under this program the velocity change was on the order of 20 ft/s which is small compared to the nominal impact velocity of 1500 ft/s.

Relative to stress wave considerations during a straight ballistic impact event, the interactions (surface tractions) are dependent on the stress fields set up within the target media and in the penetrator (generally secondary). These stress waves propagate according to the laws of wave transmission out into the semi-infinite half space of the target media. When this half space is reduced in size, as it is for RBT, the stress waves reflect from these boundaries and after returning to the surface of the penetrator, modify the existing surface stresses. Of interest in the assessment of this phenomena are:

- stress wave reflection time from free surfaces,
- extent of reflections,
- effect of reflected waves on target media (potential fracturing), and
- attenuation of reflected stress wave at the penetrator surface.

Clearly, the minimum duration of the event during which the target media appears as a half space is the time of stress wave passage to the boundary and back to the projectile. In the case of the 15.2-inch diameter RBT facility used during this program, this time is approximately 200 μsec (assuming a wave speed of approximately 7000 ft/s).

SECTION III

EARTH PENETRATORS

Two half-scale and a single 1/8 scale earth penetrator models were required for this test series. All of the test specimens were designed, fabricated and instrumented by Avco Systems Division. The two projectile designs are shown in Figures 2 and 3. The earth penetrator used in Test 1 was re-used in Test 3, to provide as many tests as possible. This EP is, with the exception of the detail in the vicinity of the two accelerometer mounts, of the same design as the penetrators used in the Avco RBT's reported in Reference 2.

All the EP models were fabricated from grade 300 maraging steel. The projectiles were hardened to a Rockwell Rc 45 (approximately 215,000 psi tensile strength). Hardening is accomplished by heating the projectile to a temperature of 925° to 950° F, for three hours and then air cooling to room temperature. The accelerometer mounts were also machined from grade 300 steel, unless otherwise indicated in Figures 2 or 3.

The nominal dimensions of the earth penetrator models and weights have been tabulated.

	Large L/D (1/2 Scale)	Low L/D (1/8 Scale)
Length (inches)	27.92	7.69
Outside Base Diameter (inches)	3.00	2.75
Wall Thickness (inches)	0.578	0.187
Weight (lbs)	39	3.7

A schematic of this projectile is shown in Figure 2 and was scaled from Reference 5. A schematic of the low L/D projectile is shown in Figure 3. Design dimensions were provided by DNA.

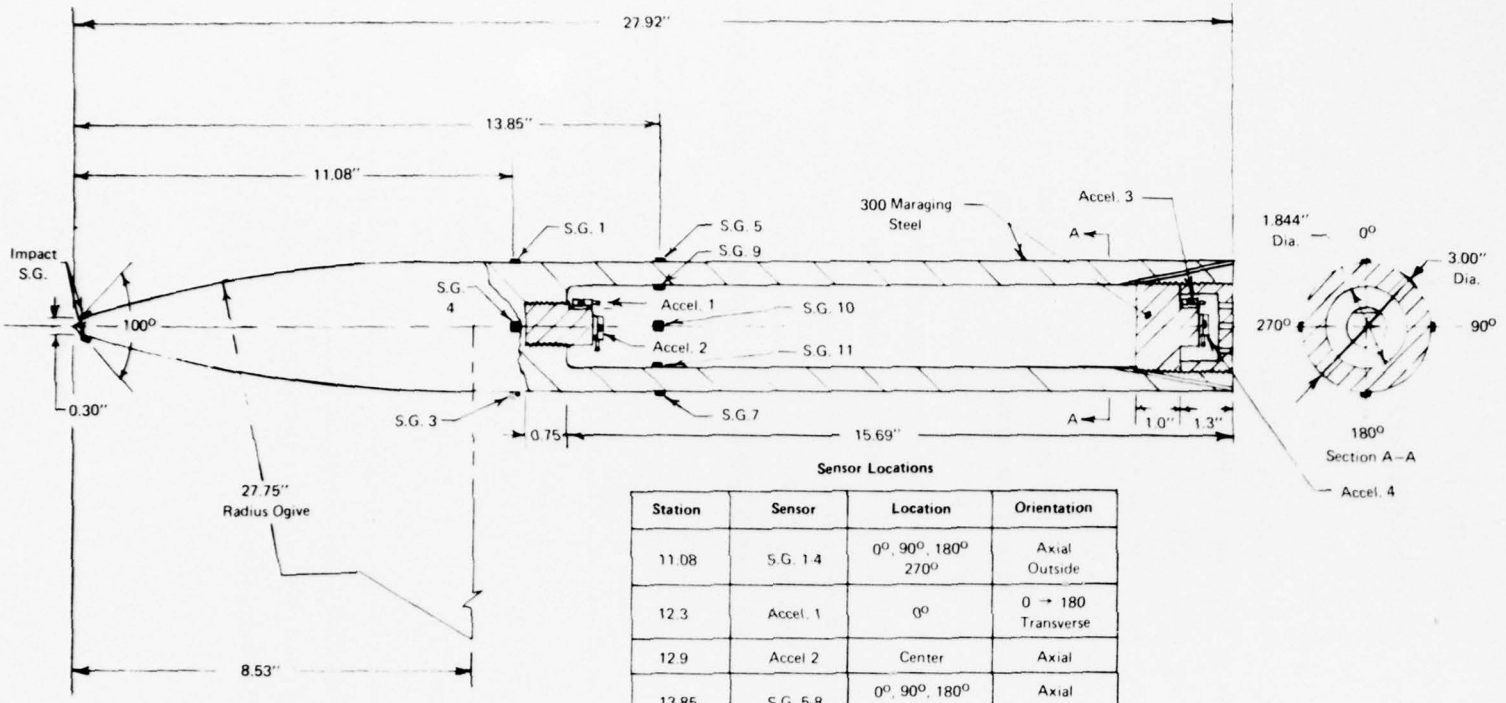

Sensor Locations

Station	Sensor	Location	Orientation
11.08	S.G. 1-4	0°, 90°, 180° 270°	Axial Outside
12.3	Accel. 1	0°	0 → 180 Transverse
12.9	Accel 2	Center	Axial
13.85	S.G. 5-8	0°, 90°, 180° 270°	Axial Outside
13.85	S.G. 9-12	0°, 90°, 180° 270°	Axial Inside
26.9	Accel. 3	0°	0 → 180 Transverse
27.3	Accel. 4	Center	Axial

Figure 2. Schematic of instrumented half scale DNA EP.

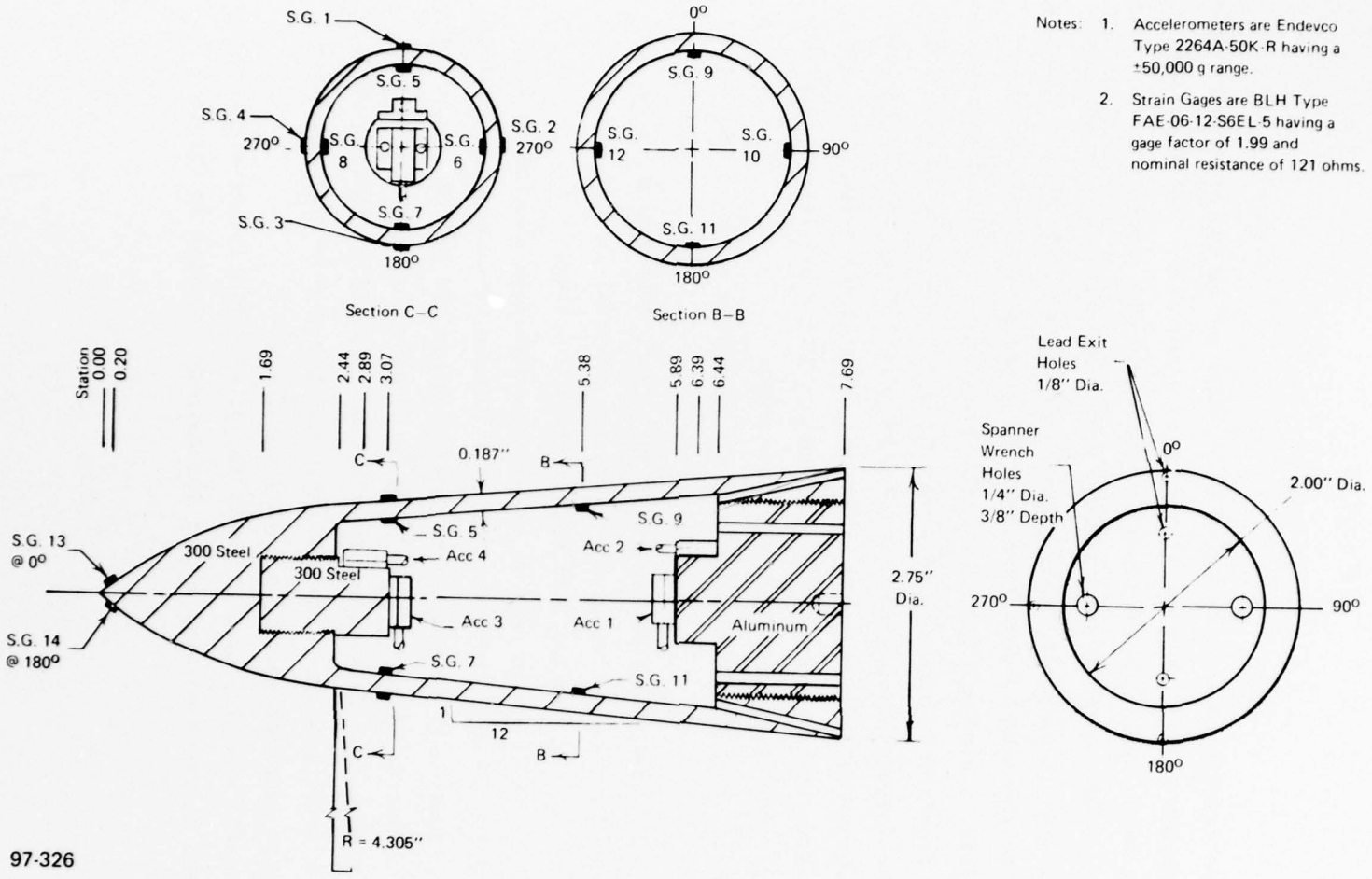

Figure 3. Schematic of instrumented low L/D EP.

SECTION IV

MEDIA TARGETS

The media targets that were explosively propelled at the stationary EP's were of two types, either concrete or compacted sandy silt. The concrete media targets were fabricated as shown in Figure 4. The concrete was contained by an aluminum canister which was machined from a standard size 16 inch O.D., 1/2 inch wall 6061-T6 aluminum tube, with a 1-1/2 inch thick 6061-T6 aluminum plate welded to the tube to form the base. Prior to pouring the concrete into the canister a one-inch thick dry sand shock cushion is used to separate the concrete from the 1.5-inch thick aluminum base. The concrete mix (Table 1) used in the targets was poured 7 to 10 days prior to the test to achieve a desired strength of approximately 4,000 psi. The actual strength of the concrete was determined on the day of the test by Universal Testing Service using a sample cast at the same time as the target.

The glacial till target material was obtained from a site in Billerica, Massachusetts.

A gradiation analysis (see Figure 5) and visual classification by the USAE Waterways Experiment Station indicates the material is classified as a Sandy Silt (SM) in the Unified Soil Classification System.

The sandy silt is contained in an aluminum canister similar to that described for the concrete targets. The soil with a water content by weight of 6.9% was placed in the container in small amounts and tamped down to obtain the desired hardness. (See Table 1.) The procedure for establishing the hardness by penetration resistance is described completely in Reference 4. Following the filling of the aluminum cups with the appropriate media the aluminum cup is machined down to a 15.2-inch diameter.

The concrete and glacial till media target characteristics are summarized in Table 1 and a sketch showing all of the targets is shown in Figure 6.

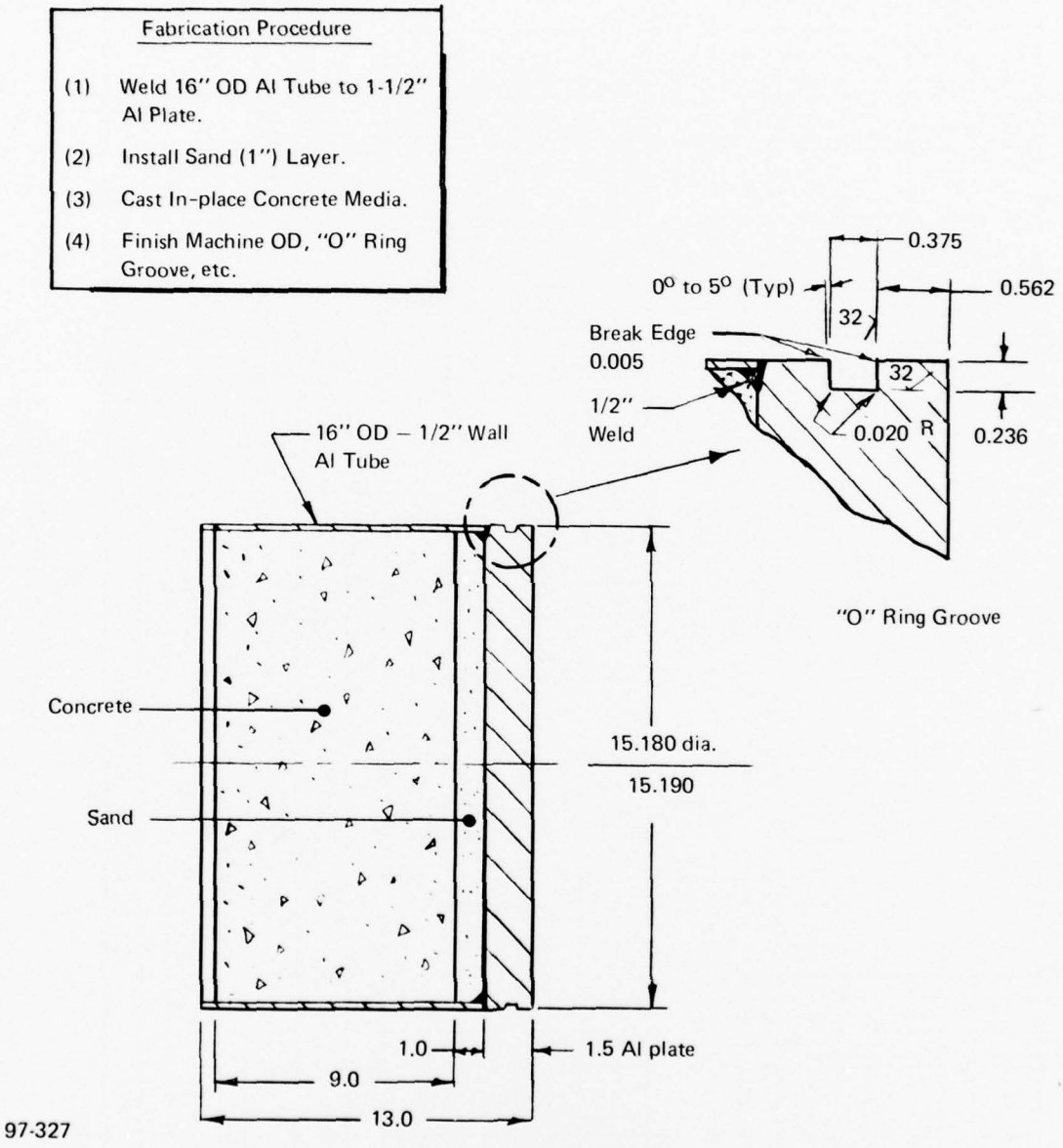

Figure 4. Schematic of thinwall aluminum – media projectile.

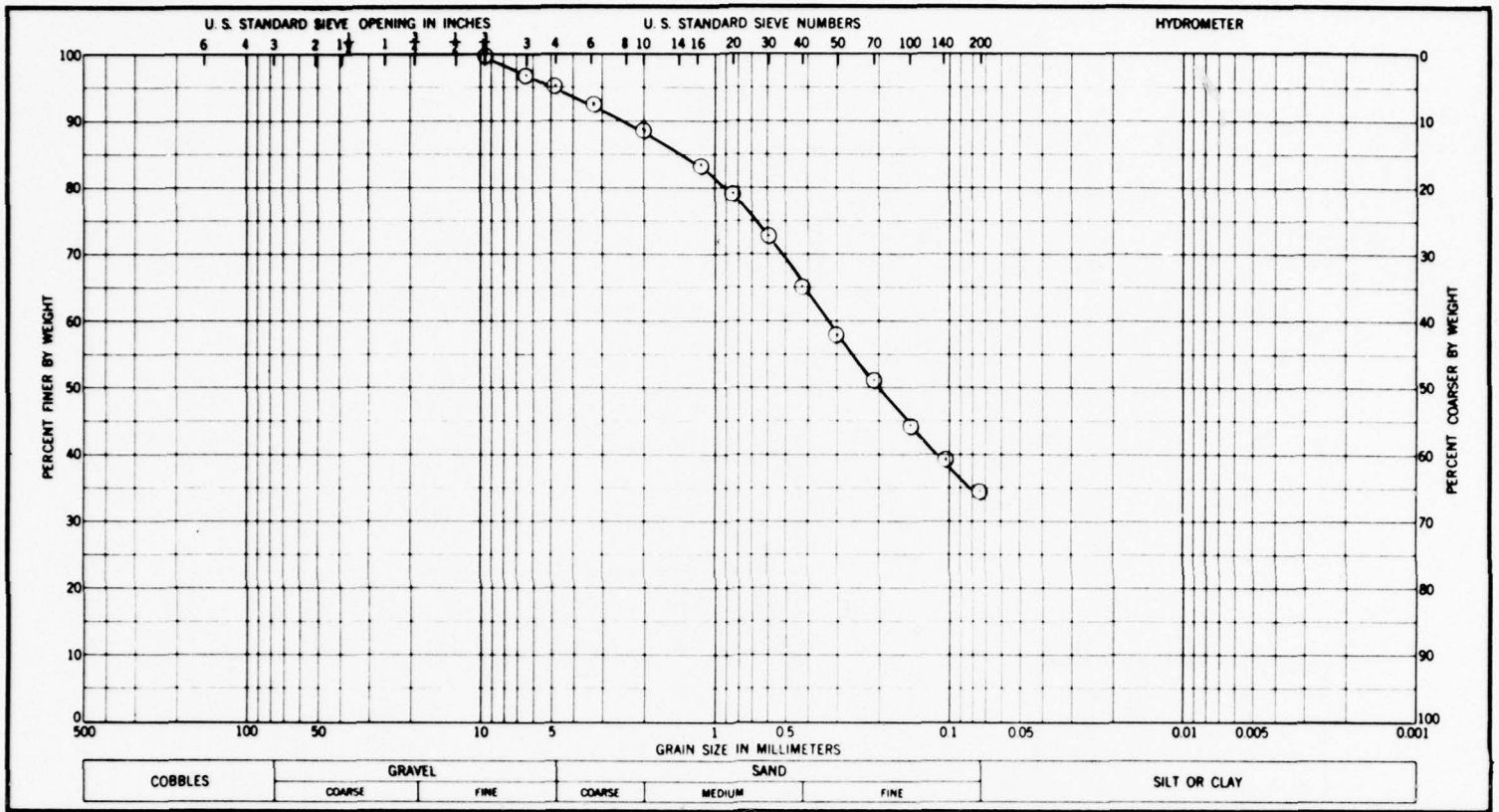

Sample No.	Elev or Depth	Classification	Nat w %	LL	PL	PI
1		Sandy Silt (SM)		NP	NP	NP
		Gray				

GRADATION CURVES

Project AVCO RBT Material

Area

Boring No. Bag

Date Feb. 9, 1977

ENG FORM 1 MAY 63 2087
97-328

Figure 5. Soil classification.

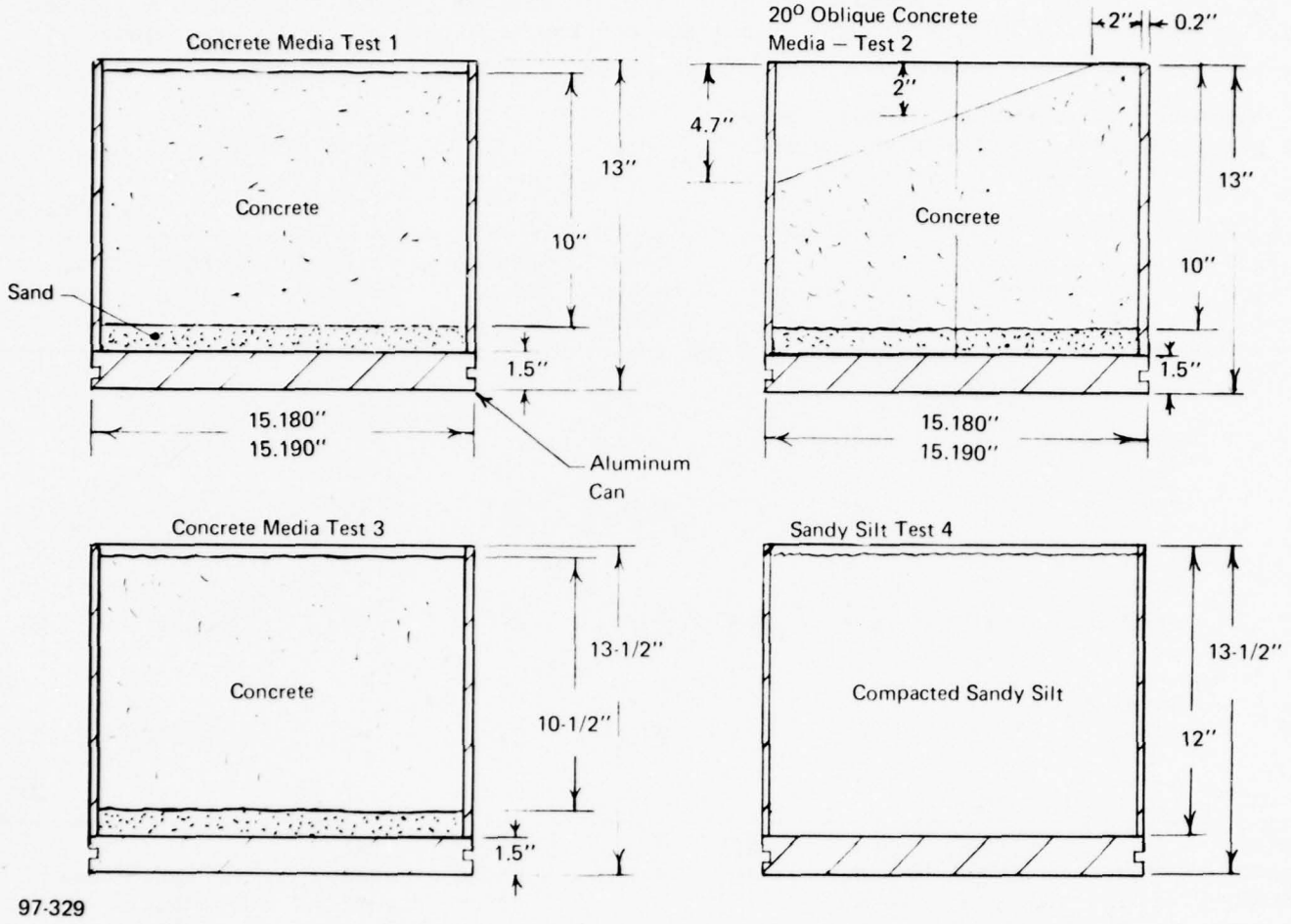

Figure 6. Target media projectile dimension.

Table 1. Characteristics of concrete and till media used for shock attenuation tests.

Test No.	Date of Test	Concrete Mix Date	Type III Portland Cement (lb)	Concrete Sand (lb)	Water (lb)	Slump (in)	Gross Weight (lb)	Net Weight (lb)	Measured Sample Strength: Date	Measured Sample Strength: Unconfined Compressive Strength (psi)
CONCRETE										
1	12/1/76	11/23/76	66	188	37.9	3.5	181	150	11/30/76 12/21/76	4740 6190
2	12/2/76	11/23/76	66	188	37.9	3.5	148	118	11/30/76 12/21/76	4580 5870
3	4/6/77	1/4/77	55	188	31.6	3.5	186	155	1/11/77 2/4/77 4/1/77	3570 5410 6650

Test No.	Date of Test	Till Mix Date	Water Content (%)	Gross Weight (lb)	Net Weight (lb)	Remarks
GLACIAL TILL						
4	4/7/77	1/4/77	6.9	204	174	Dynamic cone penetrator test indicated a penetration resistance of 60 blows/ft.

Note: Till projectile encased in polyethylene bag until 3/29/77. On this date, gross weight of till was 201.4 pounds indicating a moisture loss of 1.3% since mixed.

SECTION V

TEST CONDUCT

1. TEST FACILITY

The Reverse Ballistic tests were conducted at the Avco Ballistic Facility which is located in Otis Air Force Base, Cape Cod, Massachusetts. A photograph showing a typical ballistic test setup is shown in Figure 1.

A schematic of the 15.2-inch smoothbore reverse ballistic gun test facility is shown in Figure 7. The major components include a 10-foot long barrel section and a separate recoiling breech section. The EP model is supported by wires attached to a 4 x 4 inch wood beam mechanically attached to, and supported by the barrel section. Perturbation of the model resulting from the gun ignition shock is negligible because the barrel section does not recoil.

The EP projectile catcher details are shown in Figure 8. The catcher was filled with screened sand material and had internal dimensions of 20 x 6 x 6 feet. The soil below grade level was removed to a depth of 5 feet and backfilled with screened sand. The sides and top of the catcher were lined with railroad ties to prevent impact of the EP on concrete or steel. A double layer of ties was placed at the rear of the catcher. A total of 12 four foot cube concrete blocks were positioned to provide a containment wall around the sides and rear, and the top was covered with 6 x 6 foot steel armor plates.

2. INSTRUMENTATION

The data acquisition system is similar to that used successfully in recent DNA tests (Reference 3). A block diagram of the data acquisition system is shown in Figure 9.

Electronic sensors were installed to measure axial strain at 12 locations on each EP. In addition, four accelerometers were installed to measure "rigid body" axial and transverse acceleration at forward and aft stations, except for Tests 3 and 4, where the aft transverse accelerometer was omitted (damaged during earlier test).

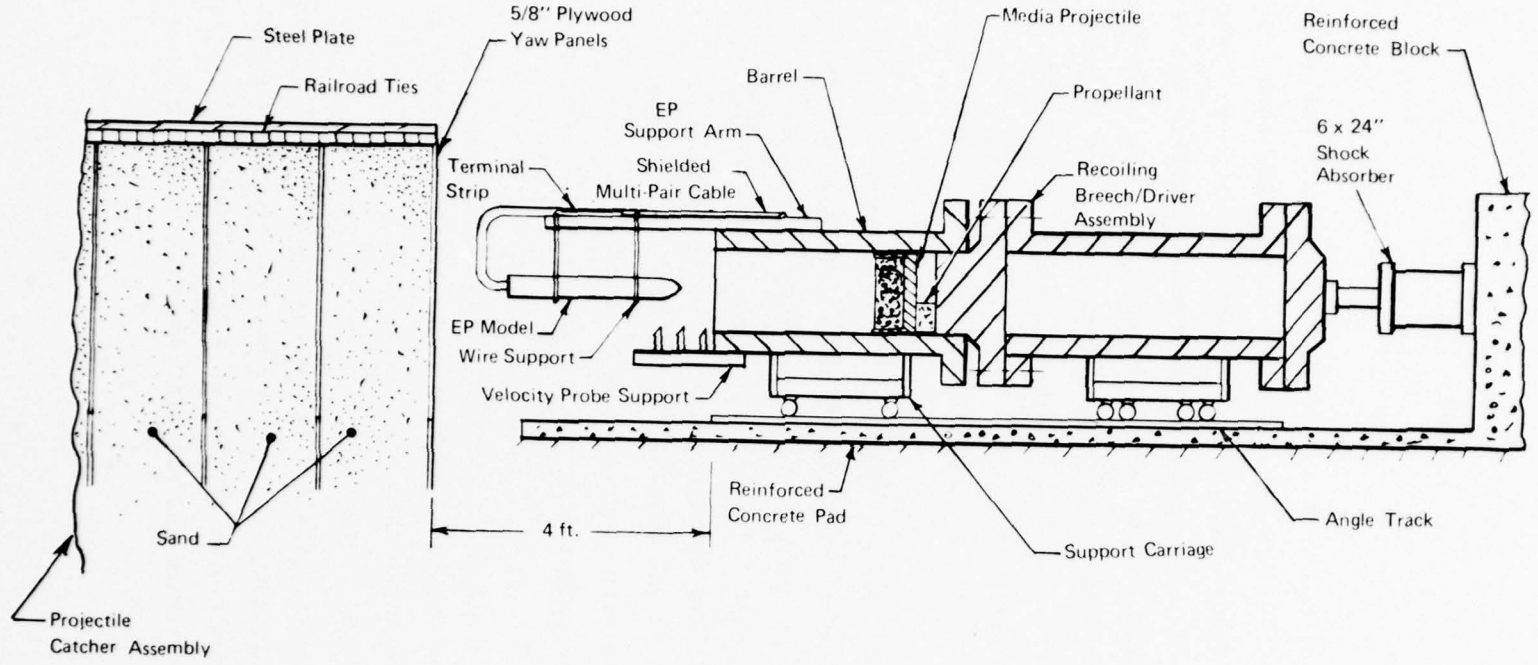

Figure 7. Avco 15.2 inch reverse ballistic test facility.

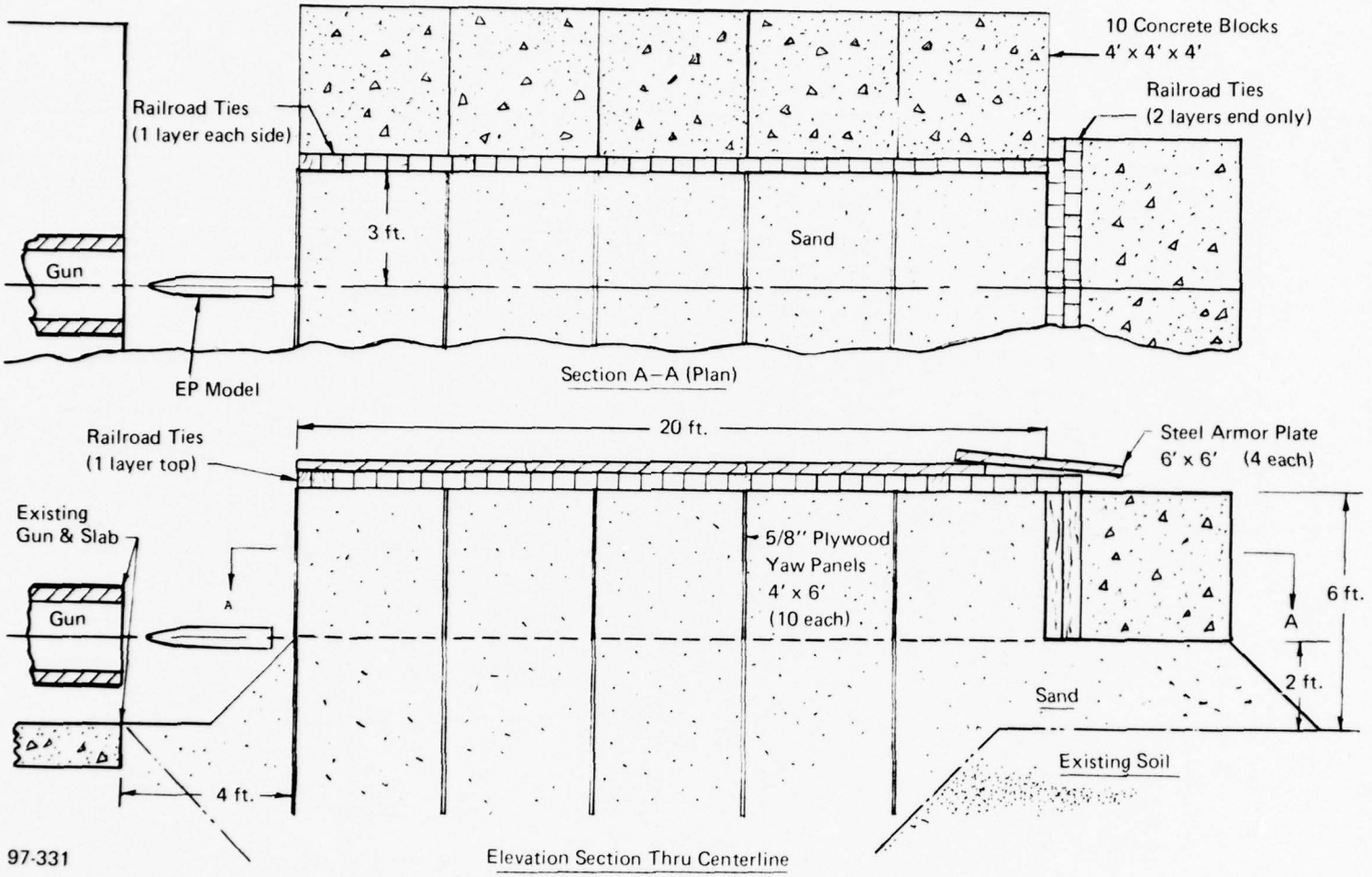

Figure 8. Projectile catcher assembly.

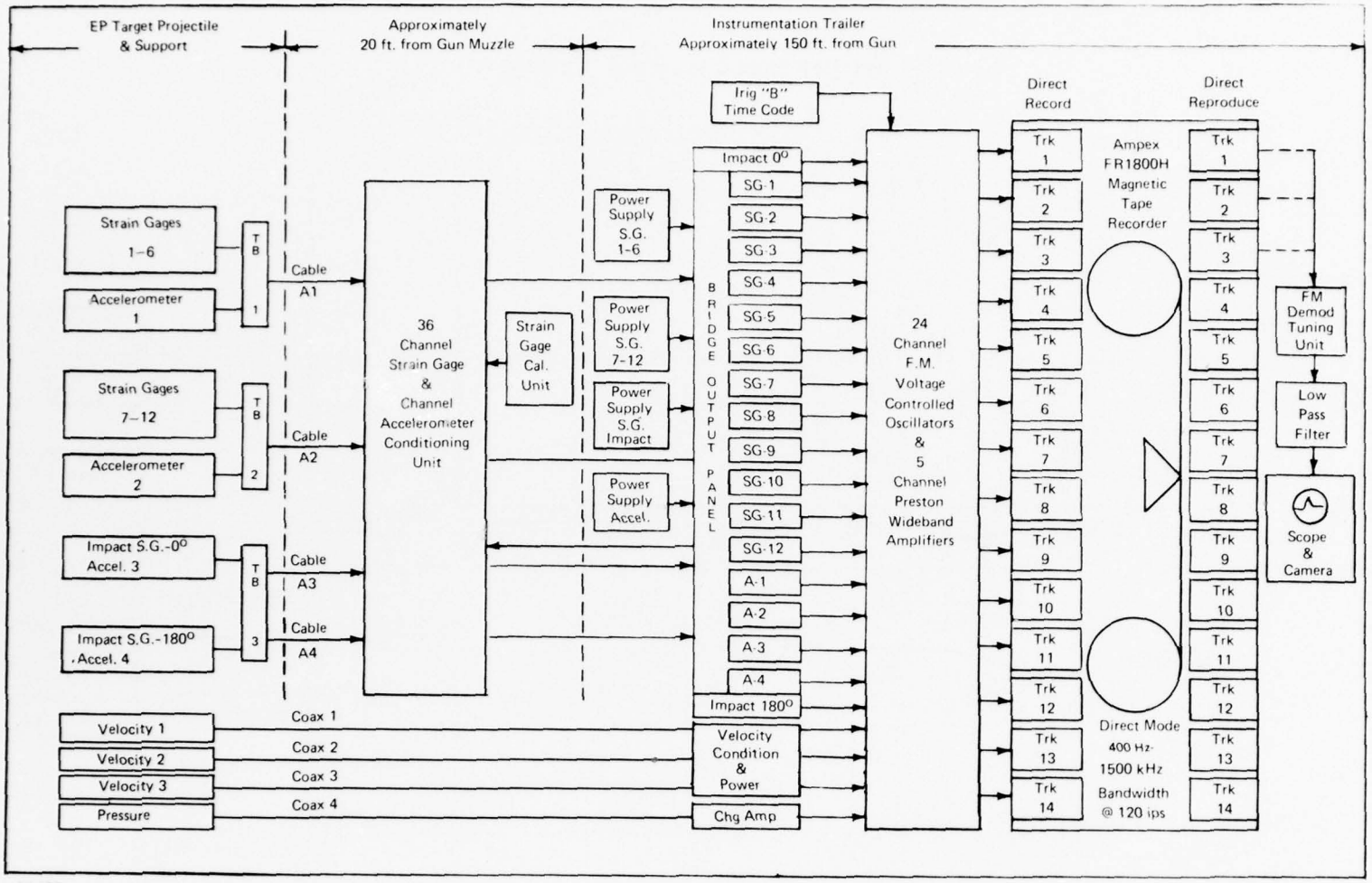

Figure 9. Reverse ballistic test data acquisition system.

Gun breech pressure was measured with a PCB 118A Ballistic pressure transducer. Velocity of the media projectiles was measured by make circuit switches and high speed motion picture cameras.

Time of impact was obtained very reliably by two strain gages located 180° apart and 0.2 inch from the nosetip of the EP. (See Figures 2 and 3.) Because of reliable impact time data, and location of all data on one recording head stack, time base errors were reduced to a minimum. Hence, it is believed that time relationships for data keyed to the impact time can be resolved to an accuracy limited primarily by the time resolution (approximately 15 to 20 μsec) resulting from the oscilloscope sweep speed used to record the data.

A schematic of the EP models showing sensor locations is presented in Figures 1 and 2.

The strain gages used were BLH type FAE-06-12S6ELI which have integral Teflon covered leads about four feet long. Gages were bonded to the EP projectile with EPY 150 epoxy. Bond layer thickness is estimated to be less than 0.5 mil. Assuming a wave speed of 0.2 inch/μsec, the time required to equilibrate the strain in the gage with strain in the steel (assuming five reverberations in the adhesive) is about 0.025 microsecond. The time required for the strain pulse to traverse the length of the 60-mil strain gage filament is about 0.3 μsec resulting in a 10/90 rise time capability of better than 0.3 microsecond.

Endevco type 2264-50K-R piezoresistive shock acceleromaters were mounted at various locations. These accelerometers have a measuring range of ±50,000 g's and a useful frequency response from dc to 30 kHz. The nominal mounted resonant frequency is 180 kHz.

The data acquisition scheme is presented in Figure 9. All strain and accelerometer data were recorded on an Ampex FR-1800H recorder. The FR-1800H recorder has 14 tracks of direct record capability having a frequency response of 400 Hz to 1500 kHz. Twenty FM record channels were frequency-multiplexed onto the first four odd tracks of the FR-1800H recorder. Each strain gage signal (resistance variation converted to proportional voltage changes) modulates a voltage controlled oscillator (VCO) to provide a deviation of the center carrier frequency proportional to the amplitude of the signal. The

outputs of five VCO's are combined to form a composite FM multiplex suitable for recording five channels of strain data onto one track of the magnetic tape recorder. The multiplexed signal, when reproduced from the tape recorder, is passed through an FM Demultiplex System which separates the various carriers, demodulates the selected channels, amplifies and shapes the resultant output so that it accurately reproduces the original signal. The bandwidth of each data channel is determined primarily by the reproduce filter bandwidth of the demodulator. A dc to 32 kHz (3 dB) bandwidth having a signal-to-noise ratio better than 35 dB is available. This bandwidth can be reduced to 20 kHz to increase the S/N ratio if the data frequency permits. Both constant amplitude and linear phase filters are available to faithfully reproduce complex as well as sinusoidal type signals.

The multiplexed channels accept low level analog voltages. Ranges of ±5 MV P-P to 10V P-P are switch selectable. Strain gage data signal lines, and the conditioning unit, were designed to provide a bandwidth commensurate with the record/reproduce capabilities. The conditioning unit and data acquisition system used for these tests was identical in response and bandwidth to that used for previous tests and is described in Reference 3.

Accelerometer outputs were transmitted directly into a wideband VCO having a dc to 500 kHz record bandwidth. Line equalization was provided to broaden the frequency response capabilities of the data lines. Line equalization increased bandwidth to about 24 kHz. Accelerometer data presented in this report was reproduced via a 32 kHz filter to reduce high frequency noise and accelerometer ringing.

Gun breech pressure, velocity make circuit outputs, and an IRIG time base were also recorded on the FR-1800 magnetic tape recorder.

The entire data acquisition system, with the exception of the conditioning unit and connecting cables, was contained and controlled from an instrumentation van located approximately 150 feet from the reverse ballistic gun. The van was protected from shock and debris by an earth berm.

Data was recovered by playback onto an oscilloscope equipped with a Polaroid camera. The scope was triggered by the first velocity probe output. In the first three tests the time of impact can be related to each data trace by using Velocity Probe 3 and impact gage signals. In Test 4 the data trace

starts at impact and because recorder skew and electronics phase shift probably contribute less than 10 μsec error, no corrections are deemed necessary.

3. HIGH SPEED PHOTOGRAPHY

A set of high speed cameras was provided to record the projectile and target position and condition immediately before and during penetration.

The photographic coverage provided high resolution position-time data for the target and media projectiles. The location of the two cameras is shown in the sketch of Figure 10. The 8 MM Hi-Cam, high speed motion picture camera (16,000 frames/sec) was positioned normal to the trajectory centerline to record position-time data with a high speed shutter installed to provide a sharp object image. The second camera was a Fastax high speed motion picture camera (5,000 frames/sec, 16 MM) and was used to observe the overall impact event. The target and media projectiles were back-lighted using a reflector and an array of FF-33 long duration flash bulbs. A sequencer was incorporated to synchronize the camera operation, flash bulb triggering, and gun firing.

4. TEST PROCEDURE

This section describes the setup and procedures followed during the actual Reverse Ballistic Tests. The photographs of the setup for Tests 2, 3, and 4 are shown in Figures 11 through 13, respectively. The EP model was suspended from an expendable wooden support by two rubber covered AWG 18 wires. Yaw and lateral sway was prevented by additional wires between the EP and other wooden beam projections attached to the bottom of the gun barrel. The model was aligned with the gun centerline to obtain less than $\pm 1/4$ degree alignment error. The lateral alignment was accomplished using a straight edge and the vertical alignment by a precise gunners quadrant.

A set of three velocity probes (normally open make switches) were attached to a steel beam which was then clamped to the gun barrel. Instrumentation leads from the EP projectile were connected to a barrier terminal strip attached to the wooden EP support arm. Shielded twisted pair wires, contained in a multipair cable, approximately 25-feet long, completed the connection between strain gages/accelerometers and the signal conditioning unit.

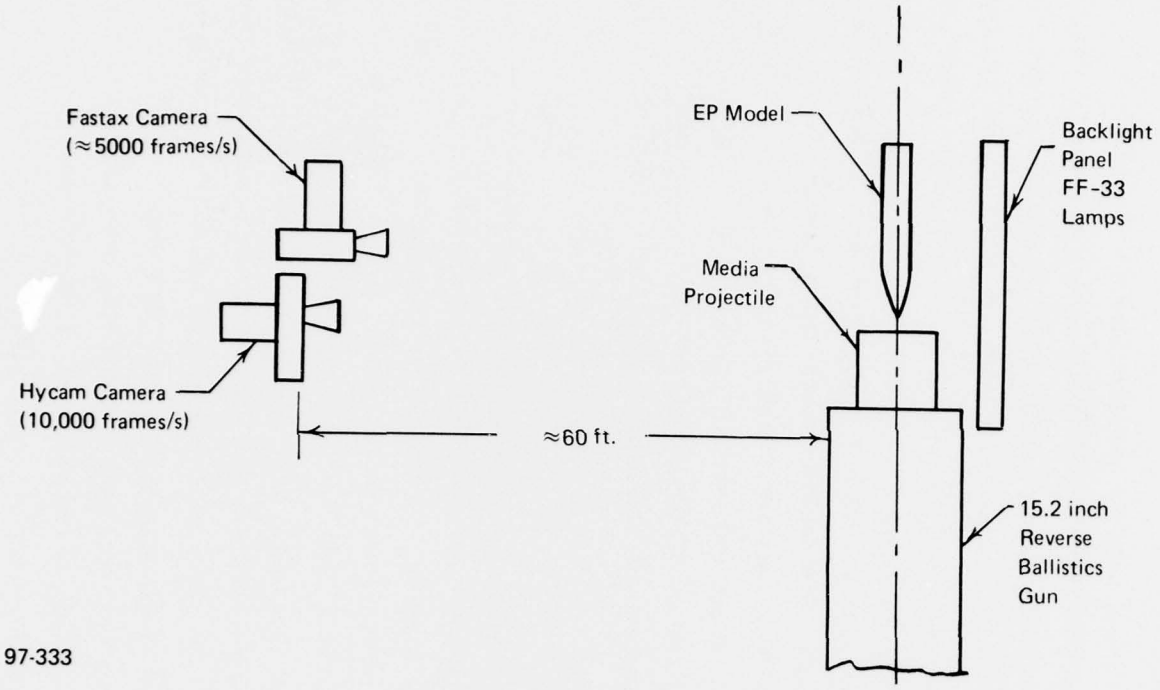

Figure 10. High speed camera position schematic.

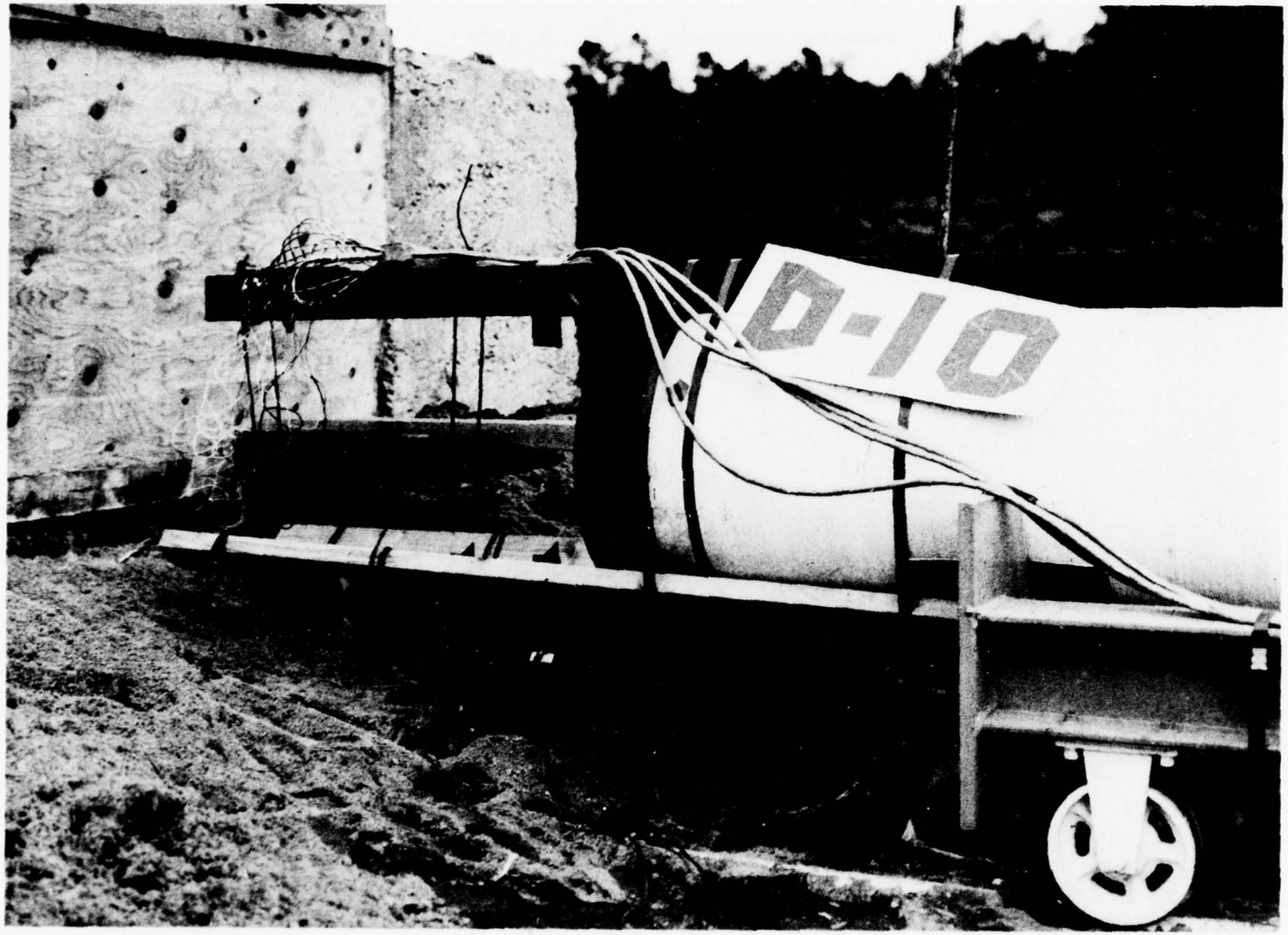

24870-D5

Figure 11. Test 2 — half scale EP test setup.

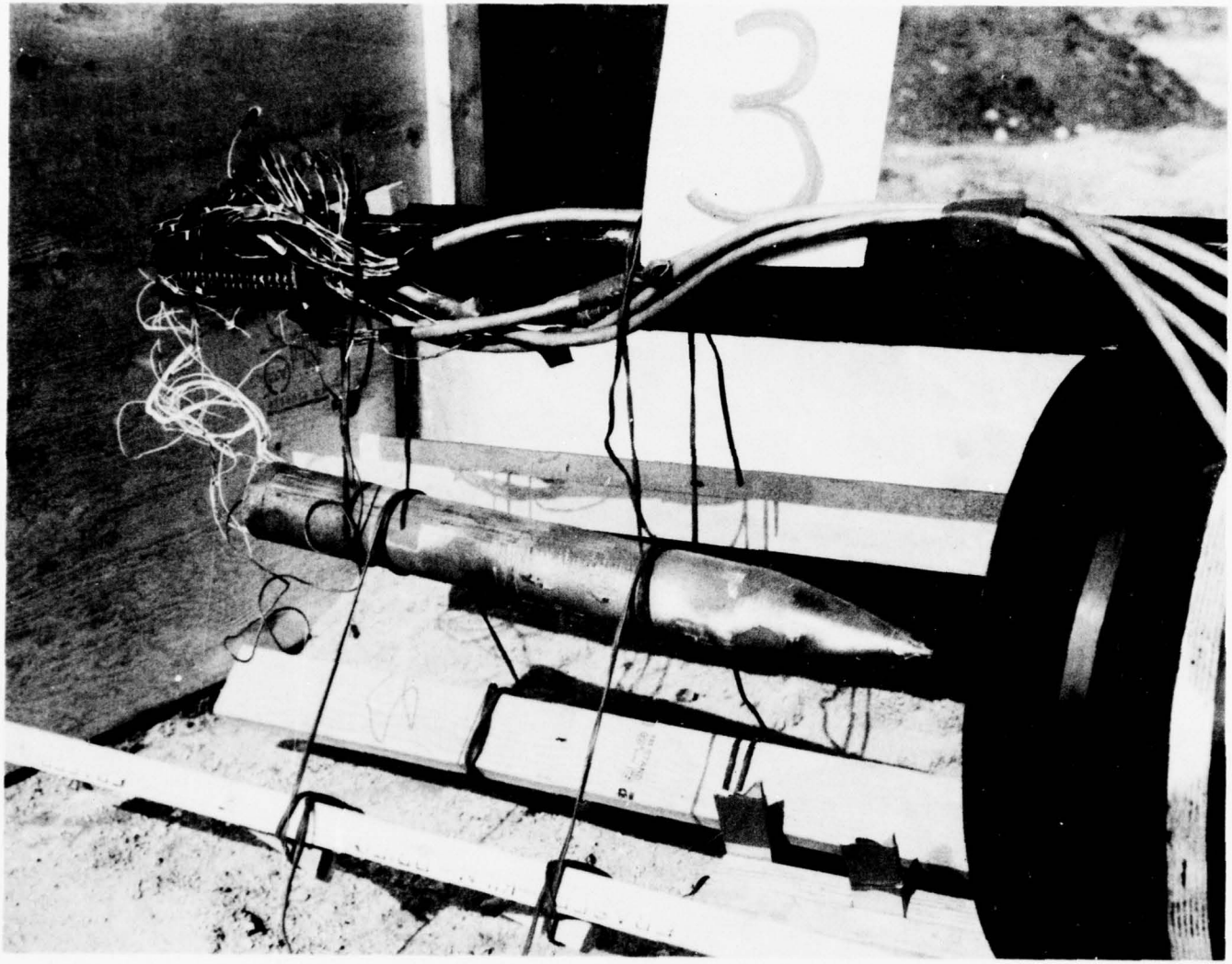

24989-D2

Figure 12. Test 3 – half scale EP test setup.

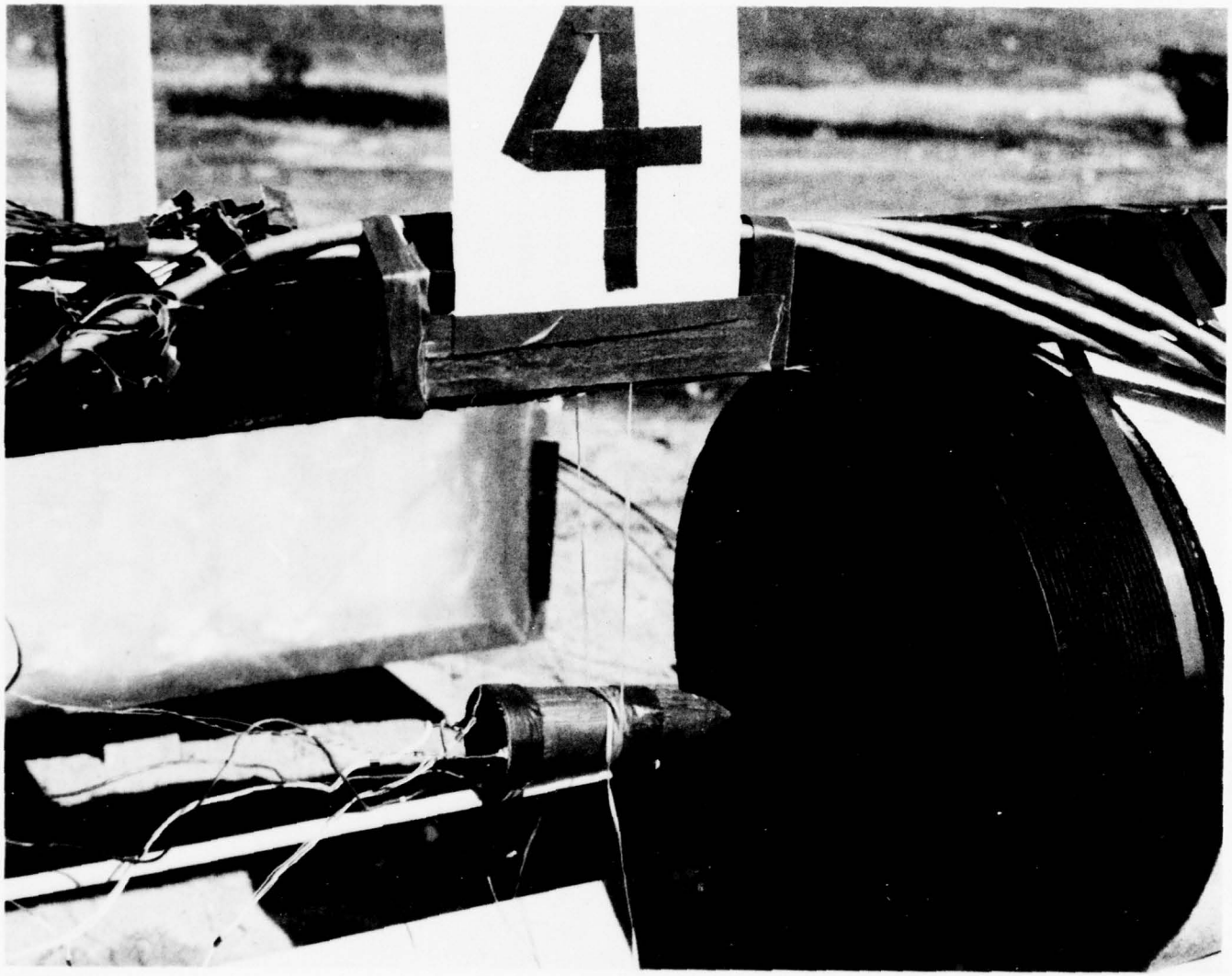

24989-A2

Figure 13. Test 4 – low L/D EP test setup.

After loading the media projectile in the gun, the data acquisition system was checked to confirm that it was functioning properly. The tape recorder band edge was set for each channel to accept the maximum expected sensor output. Then the strain gage bridges were balanced for zero voltage output and finally, simulated compression strain calibration signals were generated and recorded by shunting known resistances across each strain gage.

The propellant was loaded into the barrel and the gun was prepared for firing.

The following steps were included in the final countdown and firing sequence:

1. Check firing line for continuity.
2. Turn on tape recorder and verify proper operation.
3. Connect firing line to sequencer box.
4. Start high speed motion picture cameras.
5. When the primary camera is at the proper speed, a camera operated switch completes a circuit in the sequencer box to start a timer and apply power to flash bulbs to reach peak illumination; the sequencer automatically fires the gun.

Following the test, the catcher was disassembled to recover the EP model and the strain and accelerometer data were reproduced on-site by playback into an oscilloscope equipped with a Polaroid camera.

SECTION VI

TEST RESULTS

A brief summary of the post test parameters is shown in Table 2.

Table 2. Shock attenuation test results summary.

	Test #1	Test #2	Test #3	Test #4
Impact velocity (ft/sec)	1360	1290	1050	1750
EP angle of attack (deg)	0	0	5	5
Media obliquity (deg)	0	20	0	0
Strain gage reliability (%)	92	92	100	100
Average* axial strain ($\mu\epsilon$)	-900	-700	-640	-2200
Accelerometer reliability (%)	25	75	100	60
Average* axial acceleration (g)	8000	5000	5000	40000
Average* transverse acceleration (g)	No Data	1000	3000	20000
Concrete media strength (psi)	4740	4600	6650	N/A

In general the quantity and quality of data obtained from the four tests was very good. Strain data was recovered from 46 of the 48 gages installed and apparent response data was recorded for 10 of the 18 accelerometers installed. The response data appeared to be well within the system response limits, wherein signal amplitude and phase are accurately reproduced. The basic FM noise level was typically 2 percent rms or 8 percent (peak to peak) of peak band edge. In some cases, transients induced relatively minor (noise-like) responses 200 to 400 μsec before impact. This is believed to be caused by either thermal and mechanical effects of the pressure wave preceding the media projectile on the small (0.008-inch diameter) strain gage leads, electrical effects caused by gas ionization, or charge/discharge of media

The data obtained is only credible for a limited time period because of wave reflection from media surfaces or removal of exterior gages during penetration. The internal gages generally do not fail until the leads coming out the aft end of the model are damaged by debris at approximately one millisecond after impact.

*Average of the peak axial strain acceleration indicated at 50% penetration for all sensors with due consideration for validity of peak values (i.e., in some cases peak value of a noise pulse or ringing exceeds reported peak values). In cases where there is only one sensor (transverse accelerometer) average and peak are the same value. See Tables 4 and 5 for peak values.

A chronology of events is summarized in Table 3 which can be used to analyze the results of the acceleration and strain data in Sections 6.2 and 6.3.

1. IMPACT CONDITIONS AND VELOCITIES

The purpose of this section is to discuss the relevant parameters before and during impact of the target and the projectile. The distance from the end of the muzzle of the gun to the tip of the projectile, and the velocity as determined from either the high speed cameras or the velocity probes is discussed. In addition the condition of the projectile and target during impact are also described.

The first test was conducted at a normal impact, i.e., zero degree obliquity and zero degree angle of attack. The EP projectile nose was located 8.4 inches from the gun muzzle and at the time of impact the concrete media velocity was determined to be 1360 ft/s by the electrical velocity probe circuit. There were no redundant velocity data available from the high speed cameras because of a camera timer malfunction. Inspection of the post test condition of the target canister base plate showed an off-center penetration of approximately 1.5 inches which indicates a change from the 0^{o} angle of attack during penetration. This may be caused by the breakup of the concrete which would result in a different loading on the projectile. One potential cause for concrete failure is a misalignment of the velocity probes which project into the path of the projectile canister.

Following the test, the residual location of the EP model indicated penetration into less than four feet of sand, and the projectile had turned approximately 180^{o} with the nose oriented toward the rear of the catcher. The post test condition of the model and media container base plate is shown on Figure 14.

Because the EP in Test 1 was to be refurbished with exterior strain gages and reused for Test 3, the post test condition of the internal strain gages and accelerometers was determined. The interior strain gages, 9 through 12, located at Station 13.85 survived without damage and were reused for Test 3. Accelerometers 1 (S/N AF 94E) and 3 (S/N AG 68E), both transversely oriented, survived. Accelerometer serial number AG 68E was reused in Test 3 as Accelerometer 2 (axial). Accelerometer serial number AF 94E was reused in the

Table 3. Chronology of events-shock attenuation tests.

Event	Time from Impact*			
	Test 1 (μsec)	Test 2 (μsec)	Test 3 (μsec)	Test 4 (μsec)
1. Media impacts EP nose	0.000	0.000	0.000	0.000
2. Envelopment of Station 0.2	0.012	0.013	0.016	0.010
3. Envelopment of Station 3.07	--	--	--	0.146
4. Envelopment of Station 5.38	--	--	--	0.256
5. Ogive nose completely in media (complete envelopment of EP, Test 4)	0.429	0.452	0.556	0.366
6. Complete penetration of media	0.600	0.549	0.794	0.476
7. Contact base of aluminum media can	0.662	0.614	0.873	0.524
8. Envelopment of Station 11.08	0.679	0.716	0.879	--
9. Envelopment of Station 13.85	0.849	0.895	1.099	--

*Times based on media velocities of 1360, 1290, 1050 and 1750 ft/s, respectively.

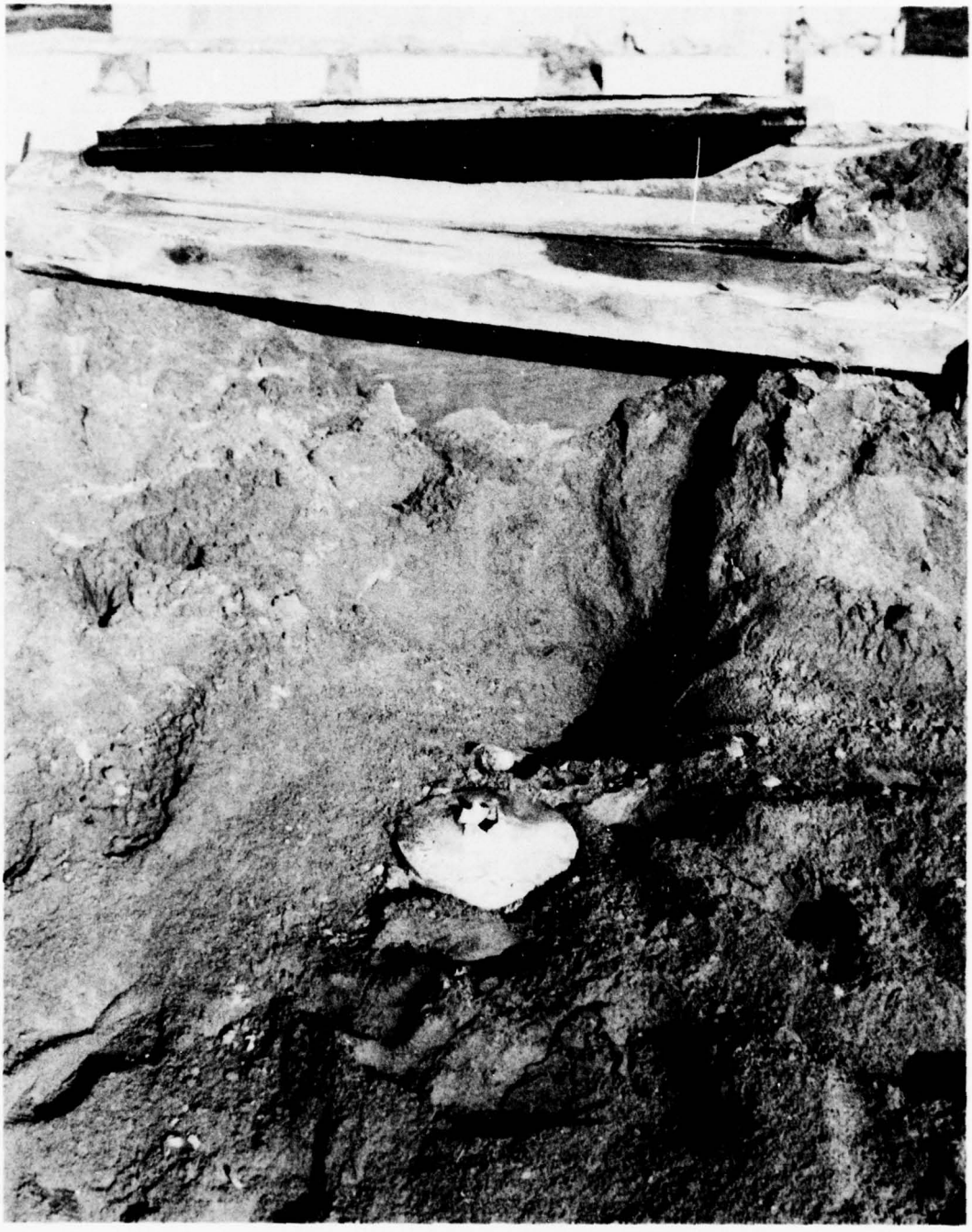

24870-C1

Figure 14. Test 1 – post test EP and media base plate position.

1/8-scale projectile as Accelerometer 3 (axial) for Test 4. The axial accelerometers (2 and 4) were damaged during the test. A post test inspection of these accelerometers (and also other failed units) indicated that the crystal had fractured into several pieces.

Test 2 was conducted with the EP at a 0^{o} angle of attack, but the surface of the concrete was at a 20^{o} oblique angle to a perpendicular with the EP axis. The concrete media was oriented in the gun so that the larger concrete mass was at the bottom of the barrel as shown in Figure 5. The Test 2 media projectile velocity was measured to be 1290 ft/s by electrical velocity probes. Again, no corroborating velocity data were available from the high speed camera because of a timer malfunction. As described in Test 1, the concrete may have been cracked near the start of penetration. This phenomenon would affect the loading distribution on the projectile.

The EP nose was located 6.1 inches from the gun muzzle prior to the test. The final position of the EP following the test indicated penetration into less than three feet of sand, as shown in Figure 15. The orientation was not altered significantly because the nose was still facing toward the gun muzzle. A post test inspection of the base plate indicated a penetration slightly off-center which again suggests the possibility of early concrete breakup. A post test examination of the accelerometers indicated that all four had fractured crystals and did not survive the test, but all of the interior strain gages survived.

The third test was conducted with a 0^{o} oblique angle concrete media impacting the half-scale EP, but with the projectile oriented nose down at a 5^{o} angle of attack. The EP nose was located 4.9 inches from the muzzle end of the gun.

High speed film data were obtained for this test and are summarized in curves describing the motion of the media projectile and target in Figures 16 and 17. Analysis of this film data indicated that the EP penetrated the concrete with a velocity of 1050 ft/s and no observed change in angle of attack until approximately 300 μsec after impact. (See Figure 18.) The concrete media integrity was maintained until after impact. A post test photograph of the EP and media container base plate is shown in Figure 19.

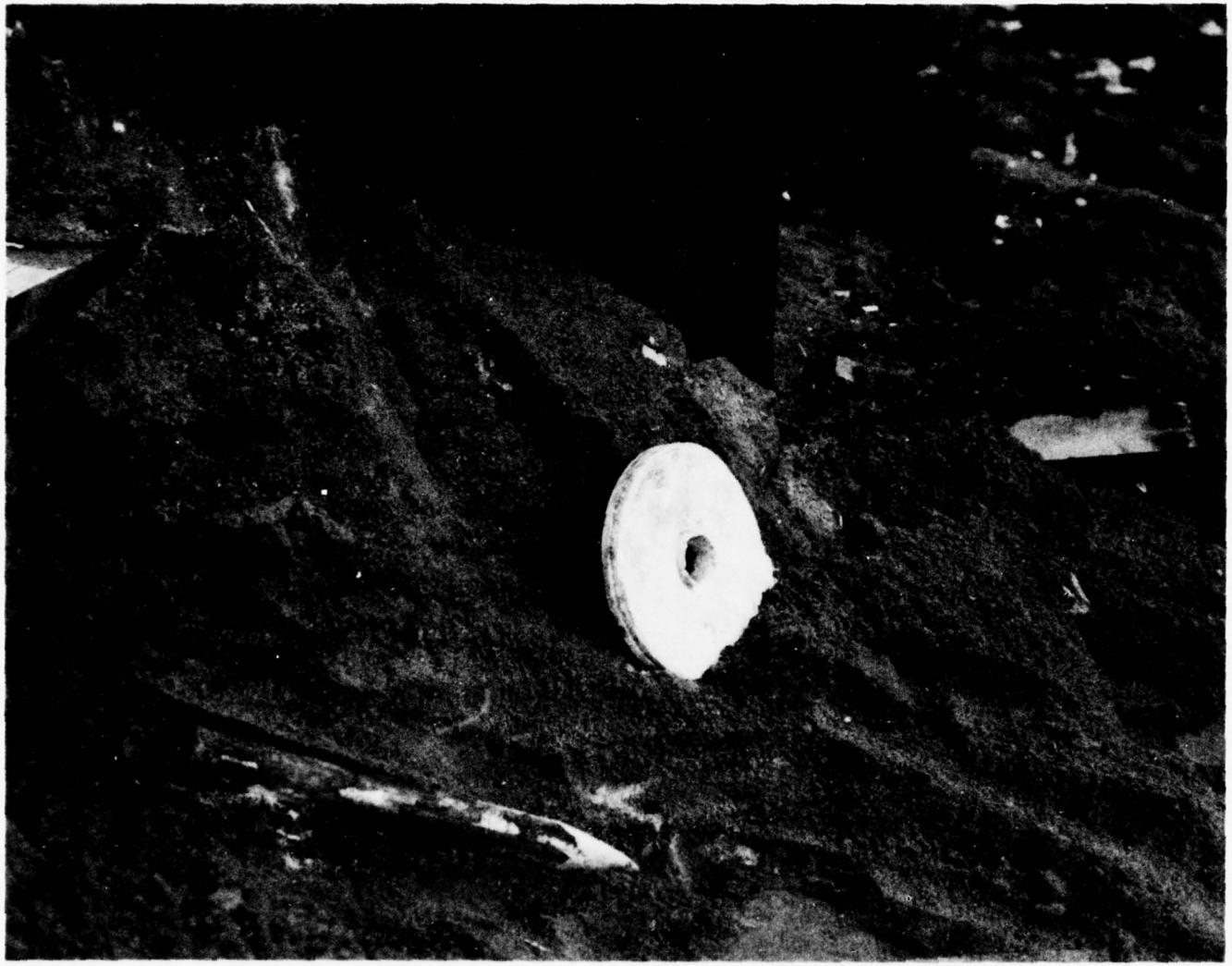

24870-D8

Figure 15. Test 2 – post test EP and media base plate position.

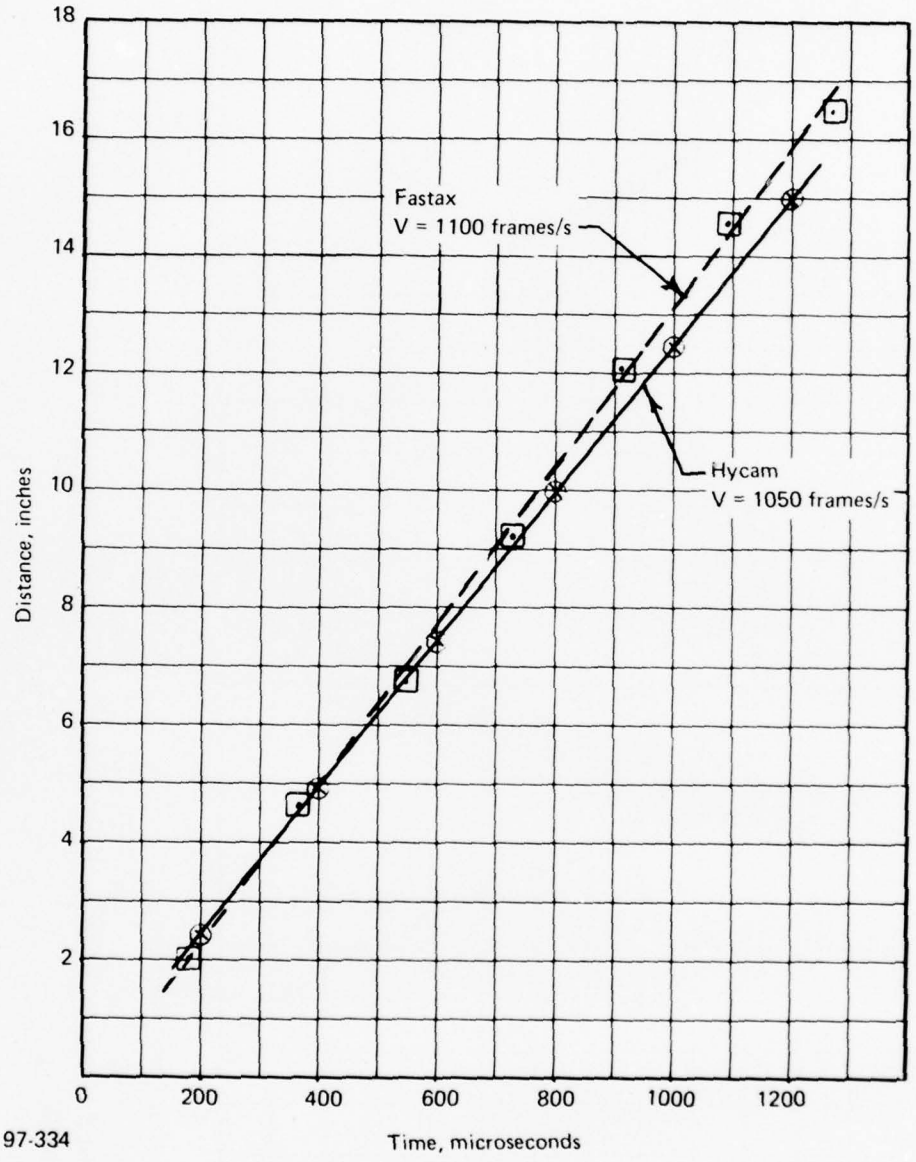

Figure 16. Test 3 – concrete media projectile velocity history.

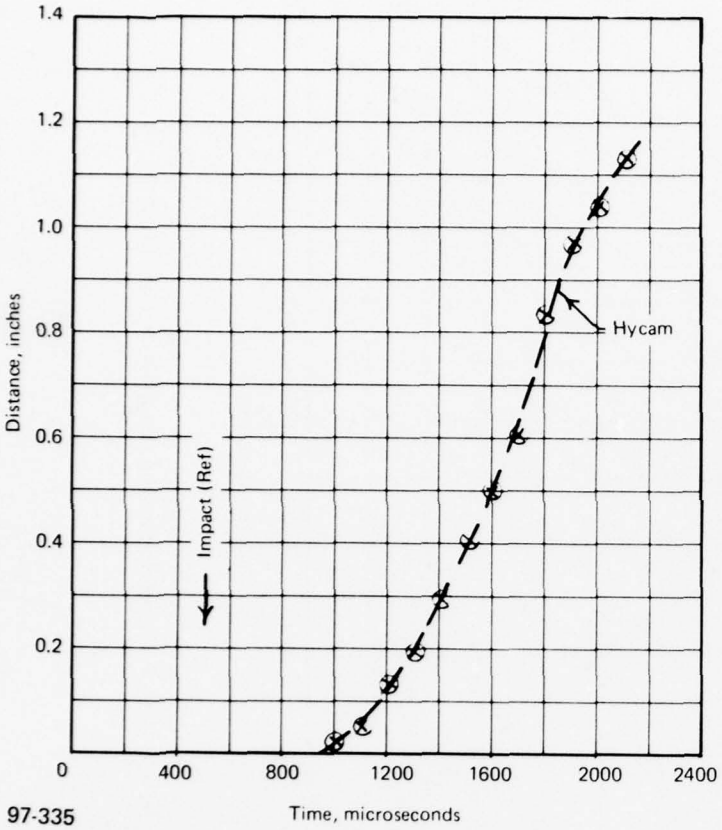

Figure 17. Test 3 – response of EP model to media impact.

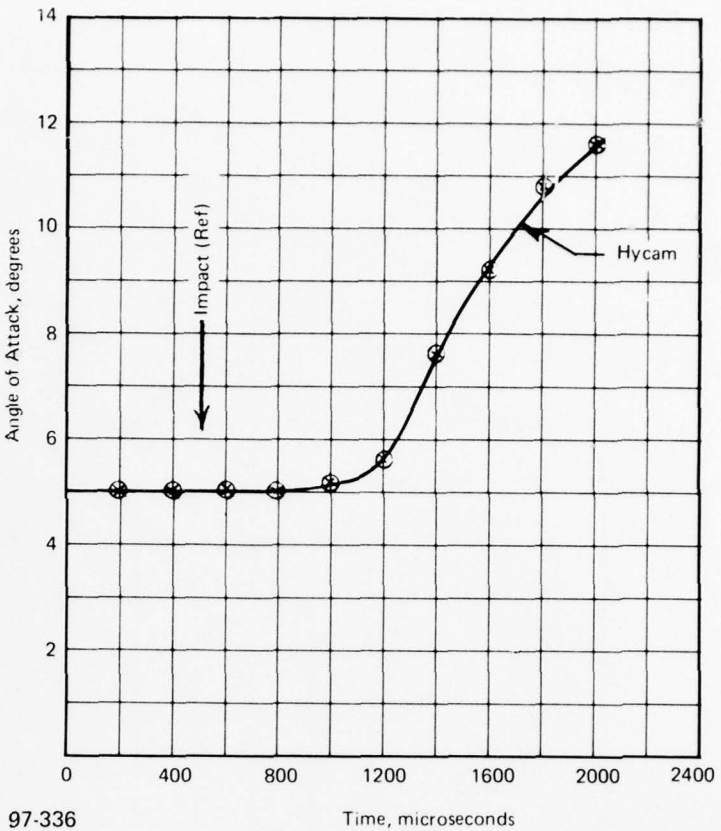

Figure 18. Test 3 – EP angle of attack history.

24989-E7

Figure 19. Test 3 – post test EP and media base plate position.

The fourth and final test was conducted with a 0° obliquity compacted sandy silt media target impacting a 1/8-scale low L/D EP model, with the model oriented nose down at a 5° angle of attack at a distance of 3.8 inches from the gun muzzle. Film velocity data for the media projectile is presented in Figure 20. Analysis of the film record indicated an impact velocity of 1750 ft/s and that the EP maintained the 5° angle of attack during initial penetration, and the till media remained intact until after impact.

Upon retrieval of the projectile (Figure 21) at the conclusion of the test it was observed to be deformed. It was determined, by reviewing the strain responses, that the failure occurred during penetration of the target cannister aluminum base plate and not during media penetration. Post test and pre test dimensional measurements of the 1/8-scale EP are compared below:

Station	0-180 Pretest Dia (in)	0-180 Post Test Dia (in)	Remarks
3.07	1.98	1.96	Strain Gage Location
5.00	2.30	2.18	Strain Gage Location
5.38	2.37	2.21	
5.50	2.39	2.23	
6.00	2.47	2.34	
6.50	2.55	2.53	
7.00	2.64	2.63	
7.50	2.72	2.72	
7.69	2.75	2.75	

The EP catcher condition following Test 4, and which is typical of all tests, is shown in Figure 22.

2. ACCELEROMETER DATA

The location of the accelerometer sensors for the half-scale EP are shown in Figure 1 and for the 1/8-scale EP in Figure 2. The accelerometer response traces for Test 1 are presented on Figure 23. Accelerometers 1, and 3 indicate anomalous data which may have been caused by the pressure wave preceding the target, possibly disturbing the lead wires that exit through

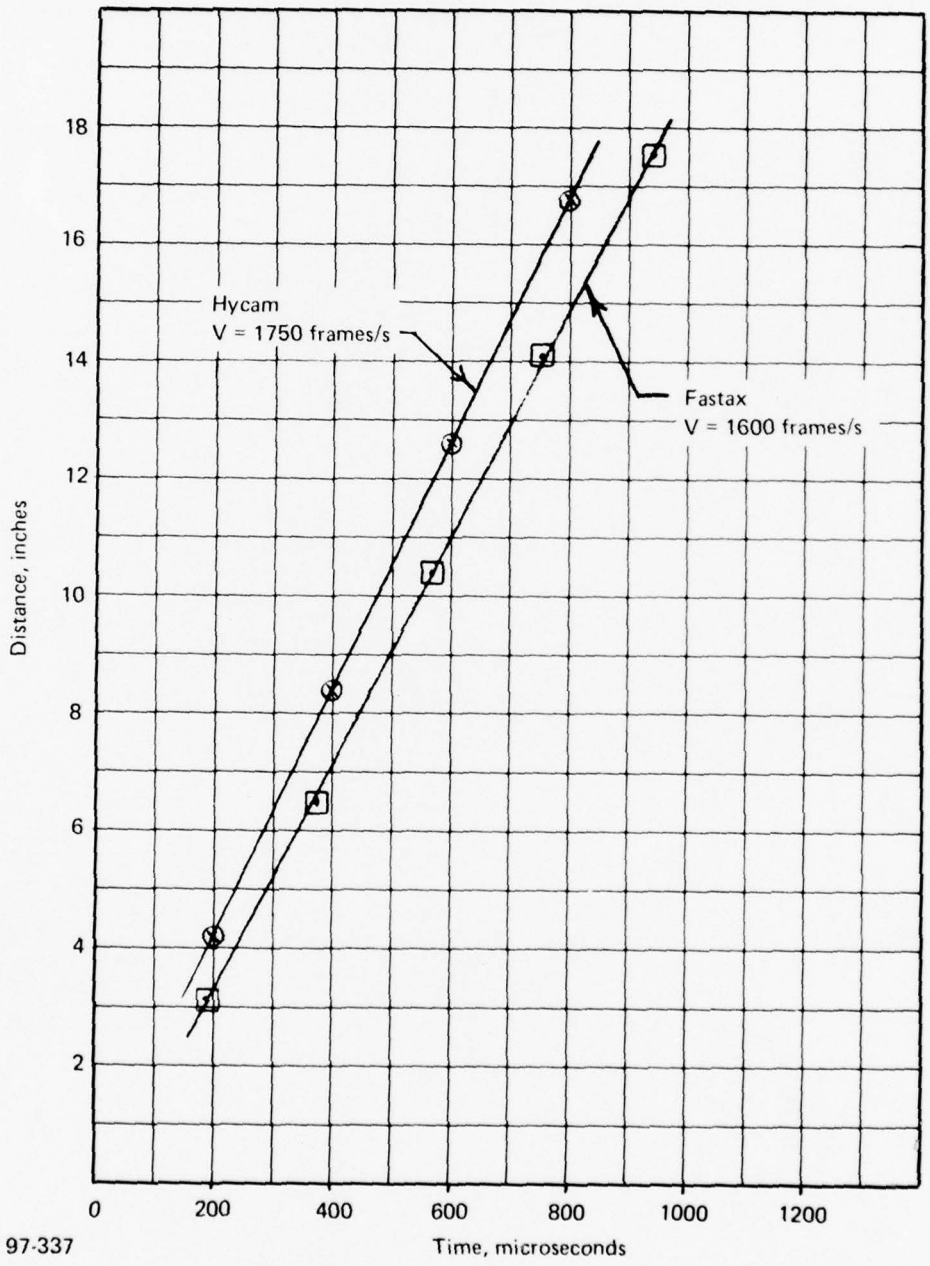

Figure 20. Test 4 – low L/D projectile velocity.

24989-89

Figure 21. Test 4 – post test EP position.

24989-B6

Figure 22. Post test catcher condition.

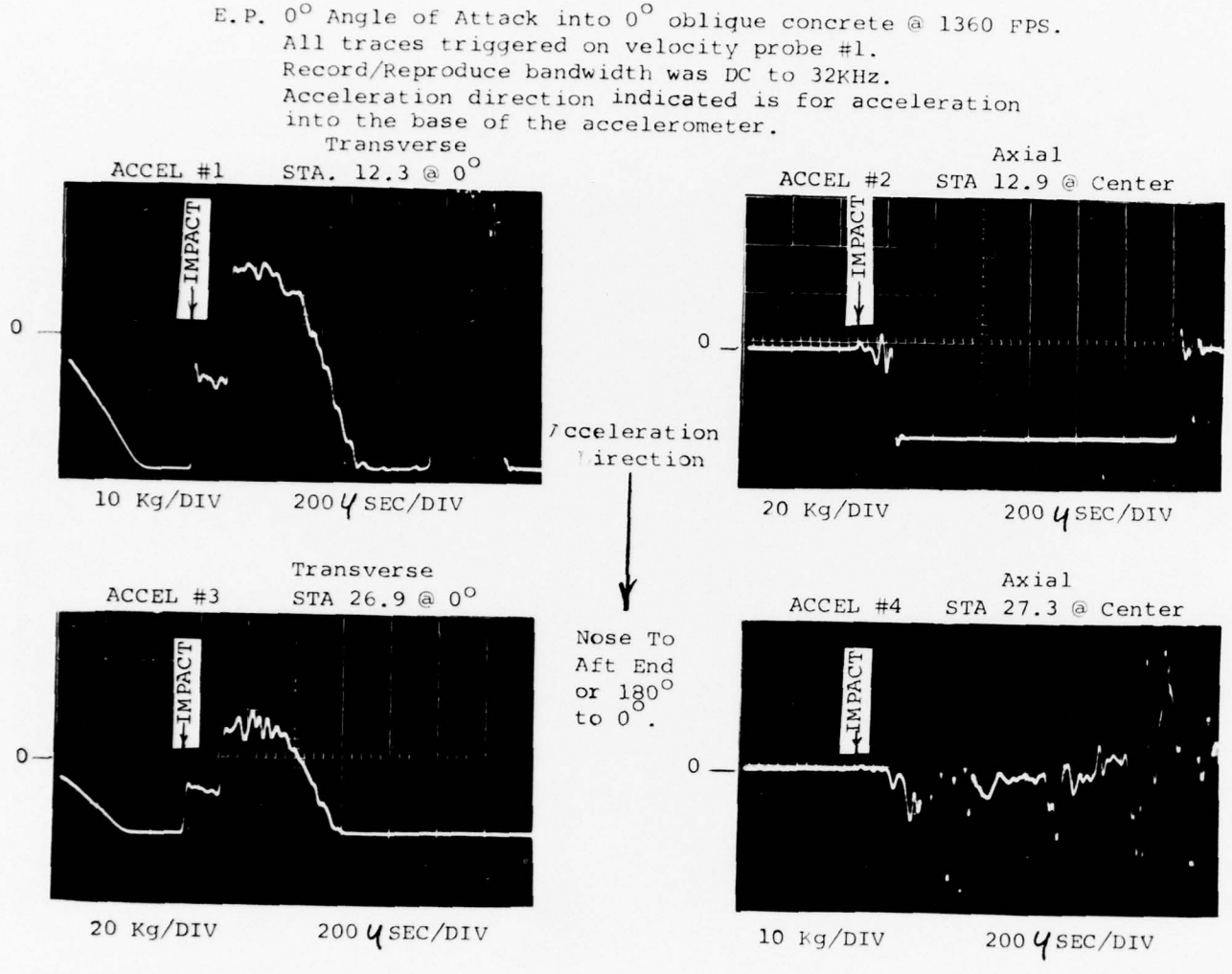

Figure 23. Shock attenuation Test 1 accelerometer data.

the rear of the projectile. Accelerometer 2 failed possibly due to either the sensor crystal or lead wire being damaged. Accelerometer 4 provided response data, although some high frequency "ringing" is apparent. The peak rigid body deceleration is estimated to be approximately 8000 g at the time the projectile has penetrated half way through the concrete target, approximately 300 μsec after impact.

The accelerometer response traces for Test 2 are shown in Figure 24. The spurious response for Accelerometer 1 from the start of scope sweep to impact is again postulated to be disturbance of the leads caused by the pressure wave. In Tests 3 and 4 the leads were securely fastened together to preclude the possibility of this re-occurring. Accelerometer 2 exhibited some high frequency "ringing" but the direction and magnitude of the rigid body response, 3000 g, appeared reasonable. The aft mounted transverse sensor, Accelerometer 3 exhibited some spurious response prior to impact, and with this accounted for, a peak rigid body level of 1000 g is indicated. The aft mounted axial Accelerometer 4 indicates a peak rigid body acceleration of 10,000 g.

In Test 3 only three accelerometers were fielded because of the failure of the accelerometers in the previous tests. From Figure 25, at 400 μsec (time to 50% concrete penetration) the rigid body transverse Accelerometer 1 indicates approximately 3000 g. In the axial direction, forward Accelerometer 2 indicates a peak rigid body response at 400 μsec of 5000 g. For the aft axial Accelerometer 4, the peak rigid body response is also 5000 g. A summary for all of the peak acceleration levels for tests 1 through 3 is presented in Table 4. In Test 4, using the low L/D projectile, the forward and aft axial Accelerometers 1 and 3, both indicate peak rigid body levels of 40,000 g at 240 μsec after impact as shown on Figure 26. In the transverse direction, Accelerometer 4 indicates a peak rigid body acceleration of 20,000 g. The rigid body accelerations are summarized for Test 4 in Table 5.

3. STRAIN DATA

The gages used to monitor the strain history on the projectile shell are located as shown in Figures 2 and 3, for the half-scale and 1/8-scale (low L/D) EP's, respectively.

E.P. 0° Angle of Attack into 20° oblique concrete @ 1300 FPS. All traces triggered on velocity probe #1. Record/reproduce bandwidth was D.C. To 32 KHz. Downward trace deflection indicates acceleration is directed into the accelerometer base (towards rear end for axial units; from 180° to 0° for transverse units).

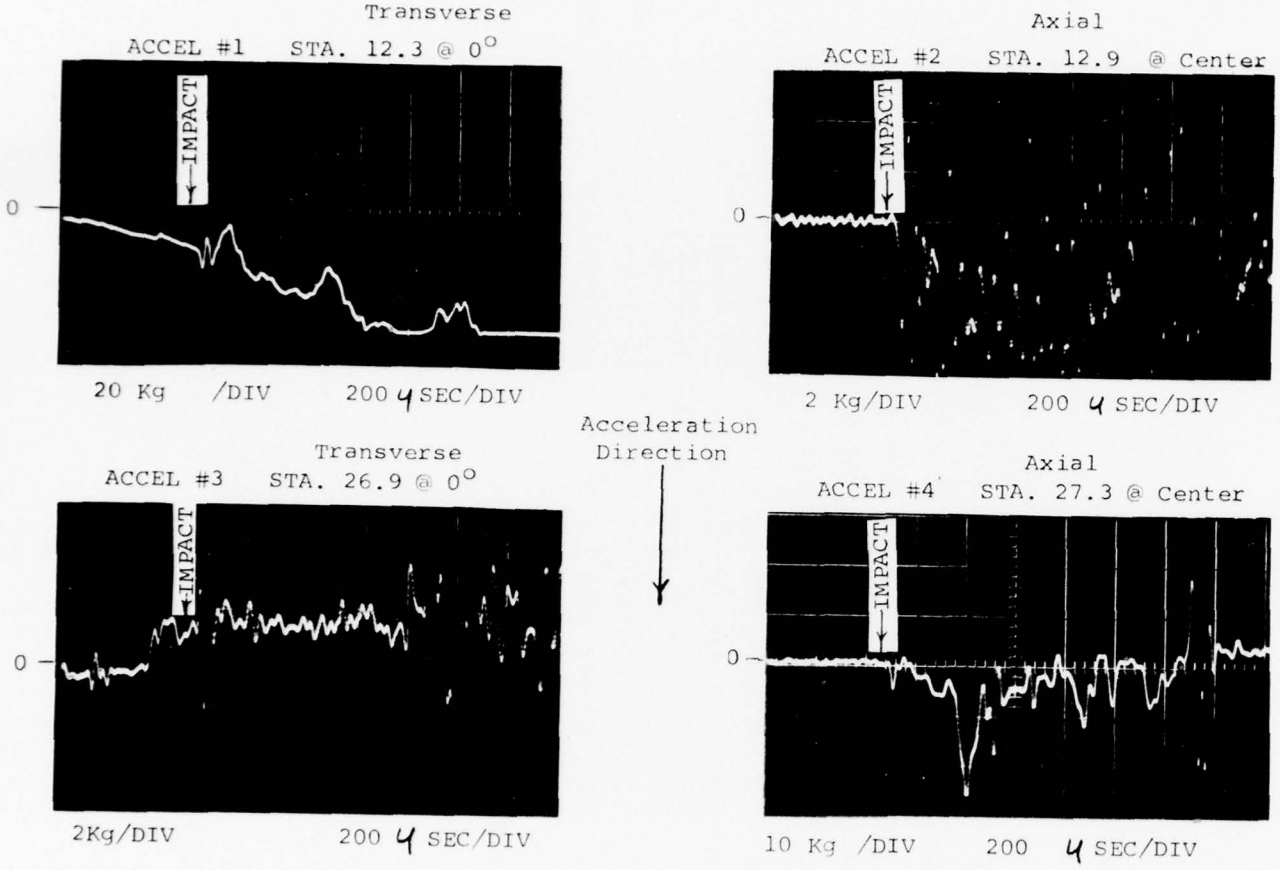

97-339

Figure 24. Shock attenuation Test 2 acceleration data.

E. P. @ 5° angle of attack into 0° oblique concrete @ 1050 FPS.
All traces triggered on velocity probe #1. Bandwidth was DC--32KHz.
Acceleration Direction indicated is for acceleration into the base of the accelerometer.

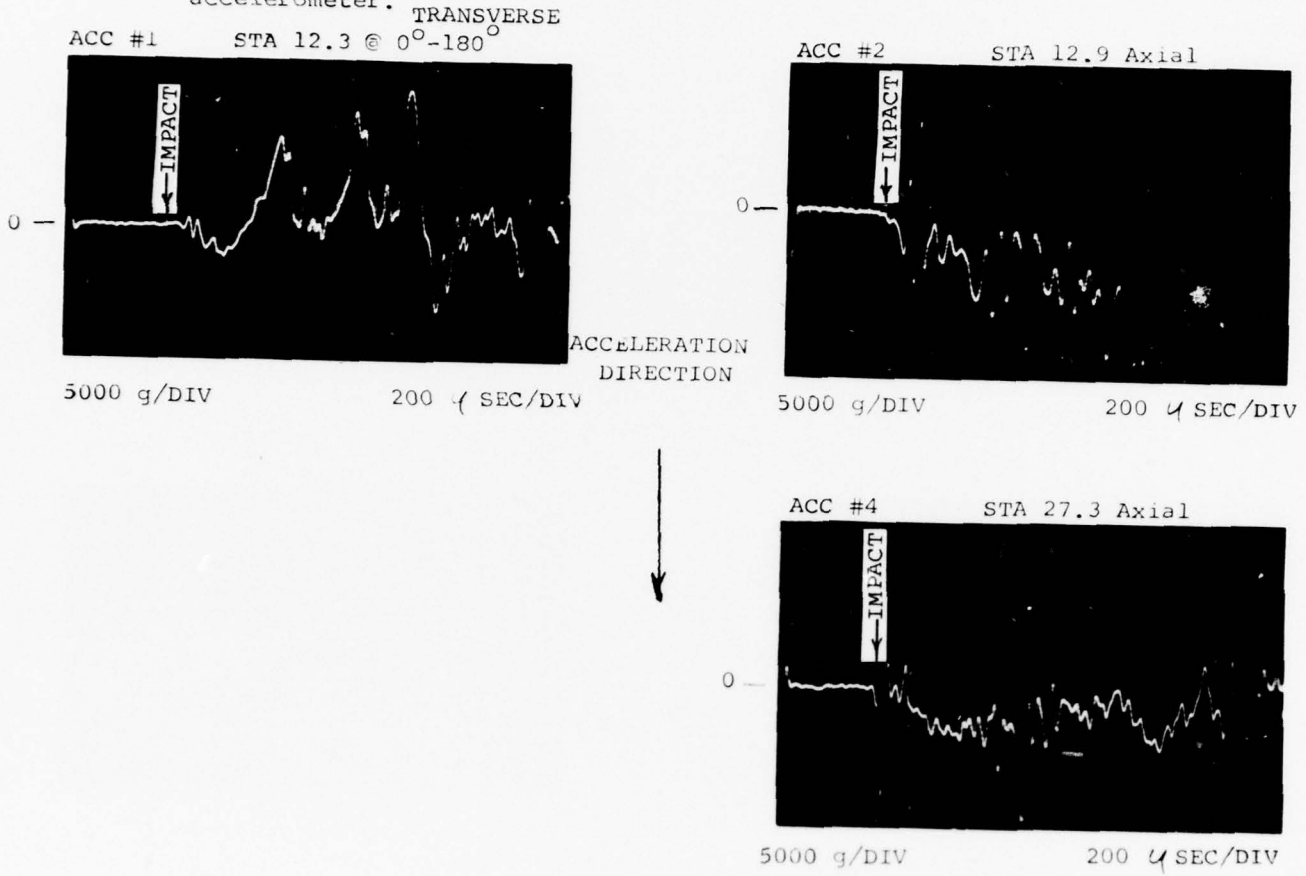

97-340

Figure 25. Shock attenuation Test 3 acceleration data.

E. P. @ 5° angle of attack into 0° oblique Glacial Till @ 1750 FPS. All traces triggered on impact S. G. #14. Bandwidth was DC--32KHz. Acceleration direction indicated is for acceleration into the base of the accelerometer.

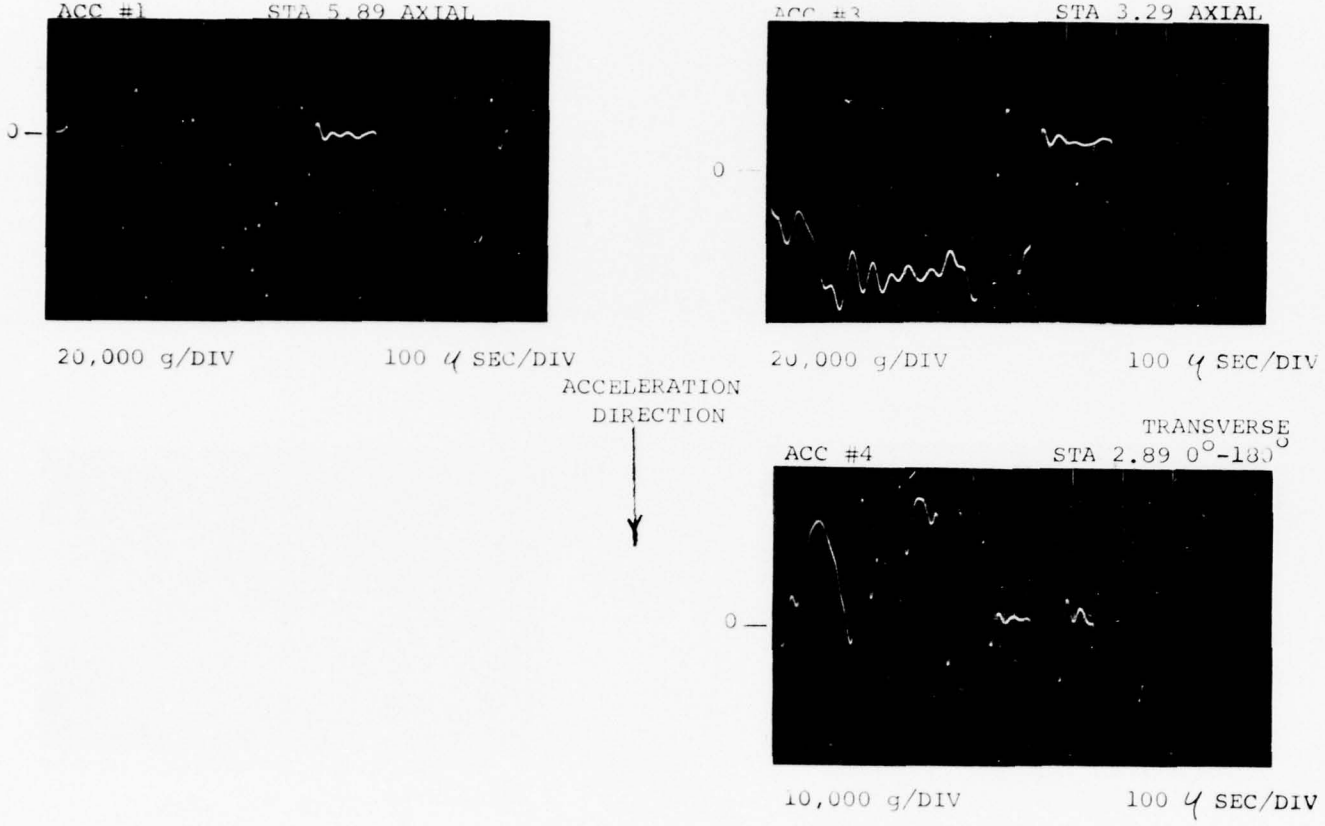

97-341

Figure 26. Shock attenuation Test 4 acceleration data.

Table 4. Data summary shock attenuation Tests 1, 2 and 3.

Sensor Type & Number	Channel Number	Station (in)	Meridian (deg)	Orientation/ Location	Time to Impact from Scope Sweep Start			Peak Strain for Approximately 50% Concrete Penetration		
					Test 1 (μs)	Test 2 (μs)	Test 3 (μs)	Test 1 ($\mu\epsilon$)	Test 2 ($\mu\epsilon$)	Test 3 ($\mu\epsilon$)
SG 1	1-1	11.08	0	Axial/Out	520	496	377	-800	> -3000	+2500
SG 2	1-2	11.08	90	Axial/Out	523	499	376	-800	-300	-650
SG 3	1-3 (1-4)	11.08	180	Axial/Out	524	500	376	-800	+3500	-3800
SG 4	3-1	11.08	270	Axial/Out	524	500	376	-800	-900	-500
SG 5	3-2	13.85	0	Axial/Out	524	500	377	-800	-5000	+2000
SG 6	3-3 (3-4)	13.85	90	Axial/Out	525	501	376	-1100	-400	-800
SG 7	5-1	13.85	180	Axial/Out	523	499	377	-1000	+4000	-3400
SG 8	5-2	13.85	270	Axial/Out	524	500	378	-1000	-1100	-600
SG 9	5-3 (5-4)	13.85	0	Axial/In	524	500	377	-900	-3000	+1100
SG 10	7-1	13.85	90	Axial/In	520	496	378	-900	-800	-450
SG 11	7-2	13.85	180	Axial/In	520	496	379	-900	+1200	-2500
SG 12	7-3 (7-4)	13.85	270	Axial/In	521	497	379	-900	-800	-700
IMPACT										
SG 13	1-4 (1-3)	0.2	0	Axial/Out	524	500	375	--	--	--
SG 14	7-4 (7-3)	0.2	180	Axial/Out	520	496	375	--	--	--
Accel 1	9 (9)	12.3	0	0 to 180 Transverse	524	500	376	No data	No data	3000g
Accel 2	10 (11)	12.9	Center	Axial	474	450	377	No data	3000g	5000g
Accel 3	11 (none)	26.9	0	0 to 180 Transverse	524	500	--	No data	1000g	None Installed
Accel 4	12 (13)	27.3	Center	Axial	474	450	378	8000g	10000g	5000g

Test 1: (12-1-76) Concrete media velocity = 1360 ft/s. 0^{o} Oblique, 0^{o} Angle of attack.

Test 2: (12-2-76) Concrete media velocity = 1290 ft/s. 20^{o} Oblique, 0^{o} Angle of attack.

Test 3: (4-6-77) Concrete media velocity = 1050 ft/s. 0^{o} Oblique, 5^{o} Angle of attack (nose down)
Parenthesized channel numbers apply to Test 3 only.

Table 5. Data summary shock attenuation Test 4.

Sensor Type and No.	Channel Number	Station (in)	Meridian (deg)	Orientation/ Location	Peak Strain ($\mu\epsilon$)
SG 1	1-1	3.07	0	Axial/Out	-1200
SG 2	1-2	3.07	90	Axial/Out	-2200
SG 3	1-4	3.07	180	Axial/Out	-4000
SG 4	3-1	3.07	270	Axial/Out	-2100
SG 5	3-2	3.07	0	Axial/In	-1300
SG 6	3-4	3.07	90	Axial/In	-2300
SG 7	5-1	3.07	180	Axial/In	-2600
SG 8	5-2	3.07	270	Axial/In	-1900
SG 9	5-4	5.38	0	Axial/In	-1800
SG 10	7-1	5.38	90	Axial/In	-1600
SG 11	7-2	5.38	180	Axial/In	-2400
SG 12	7-4	5.38	270	Axial/In	-1500
IMPACT					
SG 13	1-3	0.2	0	Axial/Out	--
SG 14	7-3	0.2	180	Axial/Out	--
Accel 1	9	5.89	Center	Axial	40000g
Accel 3	11	3.29	Center	Axial	40000g
Accel 4	13	2.89	0^{o} to 180^{o}	Transverse	20000g

Test 4: (4-7-76) Sandy Silt media velocity was 1750 ft/s. 0^{o} Oblique, 5^{o} Angle of attack (nose down).

As noted previously, the number of channels of strain data retrieved and the quality of the response was excellent. The only spurious response is found in Test 1 where at the time of impact there is a sharp spike which may be caused by a static charge built up on the media projectile and discharged upon impact. In subsequent tests the distance between the gun muzzle and projectile was reduced and this problem was apparently solved.

The strain response traces for Test 1 are presented on Figures 27 through 29. On all strain gages in Test 1, up to the time of half penetration of the concrete target ($\sim$ 300 μsec), the peak strains are compressive and range from 800 to 1100 μin/in. The peak strains for all of the strain gages are presented in Table 4.

In Test 2 with the 20° obliquity the accelerometer response traces for Gages 1 through 12 are shown on Figures 30 through 32. Gages at 0° indicate peak strain levels of 3000 to 5000 μin/in (compression); at 90° the peak strains are 300 to 800 μin/in (compression); at 180° the peak strains are 1200 to 4000 μin/in (tension); and at 270° the peak strains are 800 to 1100 μin/in (compression). The peak strains for each gage are summarized on Table 4.

For Test 3, the 5° angle of attack of the half-scale penetrator, and the strain gage response traces are presented on Figures 33 through 35. The peak strains for the gages at 0° are in tension and range from 1100 to 2500 μin/in; at 90° the peak strains are compressive and range from 450 to 800 μin/in; at 180° the peak strains are compressive and range from 2500 to 3800 μin/in; and finally the gages at 270° are compressive and range from 500 to 700 μin/in. The peak strains for each gage are summarized on Table 4.

The strain results for Test 4 due to the short length of the EP have a very limited time for data recording of the external strain gages. The forward external gages which are located $\sim$3 inches from the tip are destroyed in approximately 150 to 200 μsec after impact. For the fourth test, the strain response results are presented on Figures 36 through 38. The peak strains recorded are presented in Table 5. In summary, the gages are all in compression and at 0° indicate a peak strain range from 1200 to 1800 μin/in; at 90° a peak strain range from 1600 to 2300 μin/in; and 180° the strain range from 2400 to 4000 μin/in; and at 270° the peaks are from 1500 to 2100 μin/in.

E.P. 0° Angle of Attack into 0° oblique concrete @ 1360 FPS.
All traces triggered on velocity probe #1.
Record/reproduce bandwidth was DC to 32 KHz.

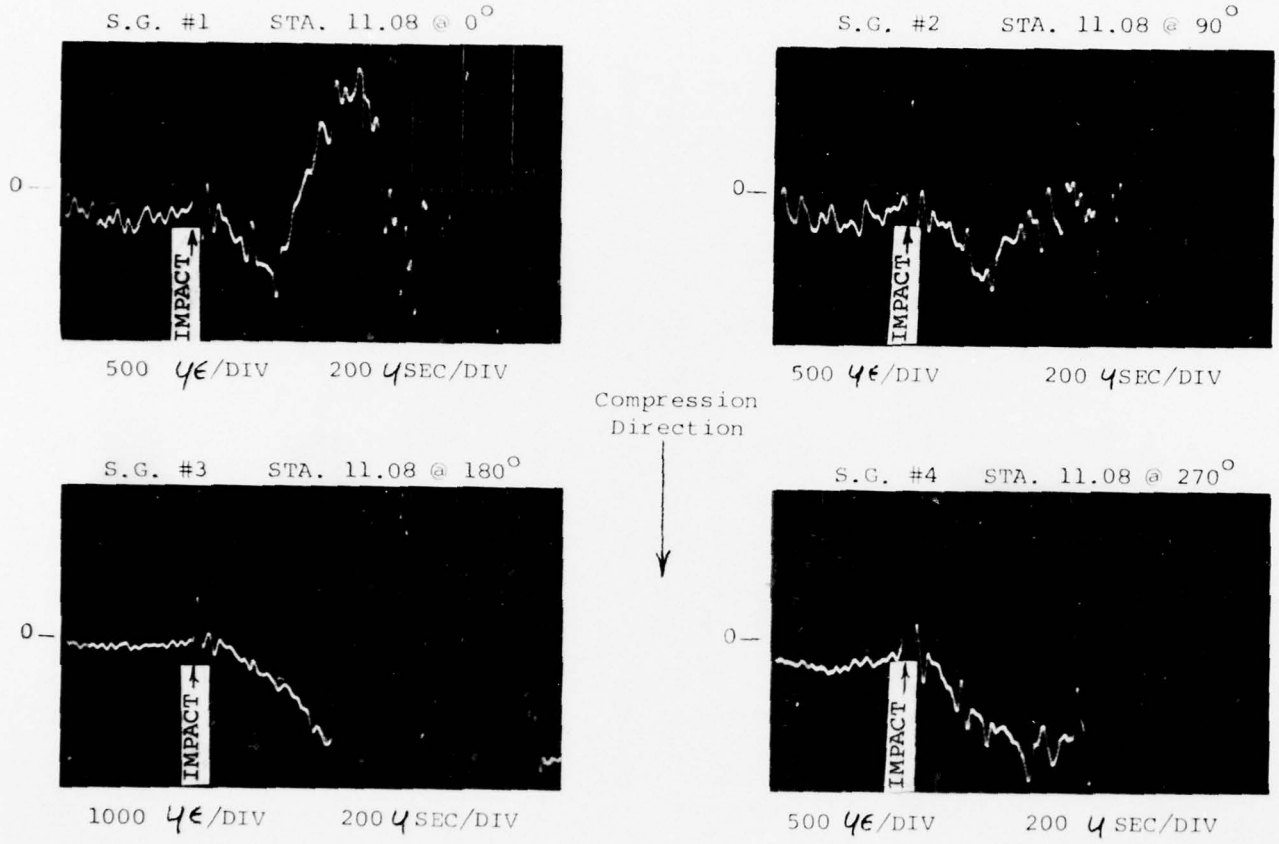

97-342

Figure 27. Shock attenuation Test 1 external strain.

E.P. 0° Angle of Attack into 0° oblique concrete @ 1360 FPS.
All traces triggered on velocity probe #1.
Record/reproduce bandwidth was DC to 32KHz.

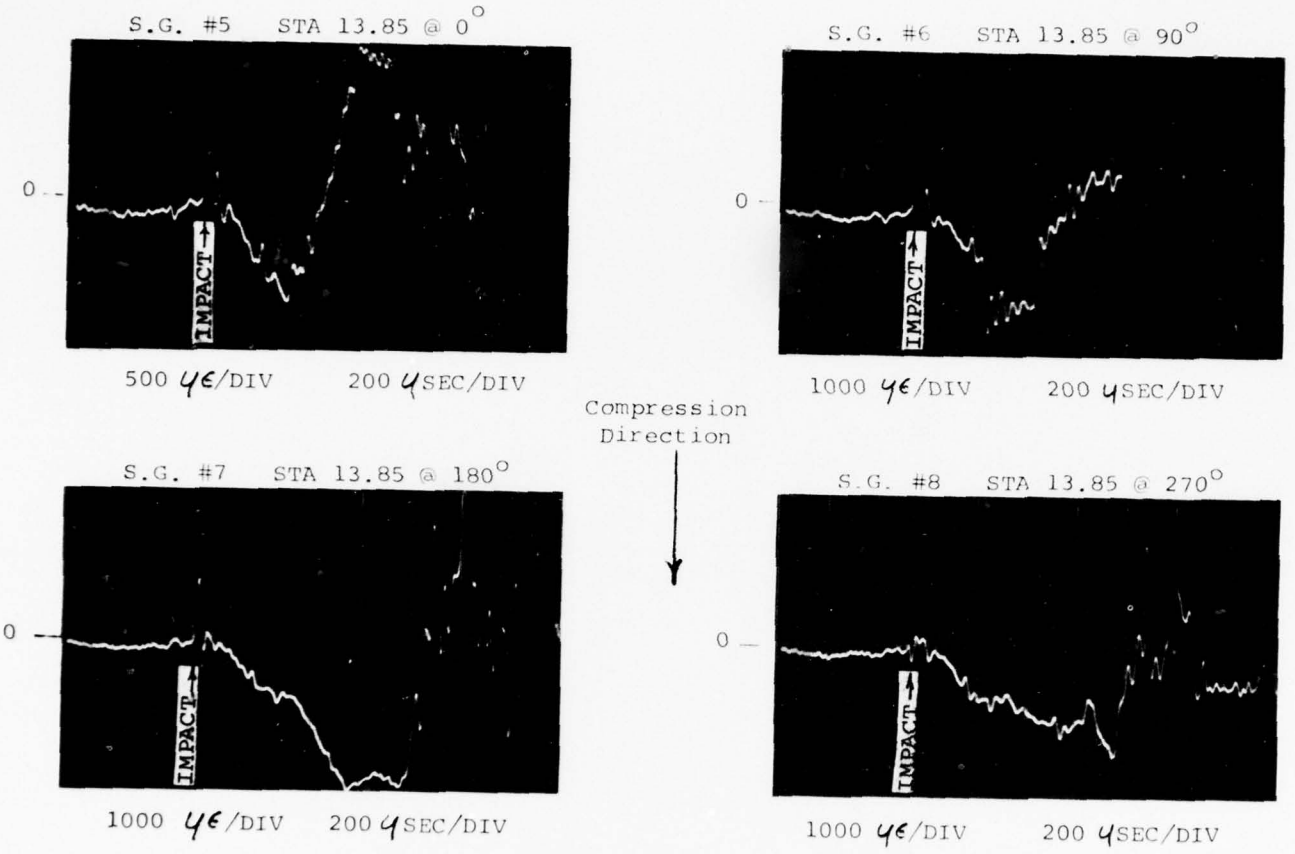

97-343

Figure 28. Shock attenuation Test 1 external strain.

E.P. 0° Angle of Attack into 0° oblique concrete @ 1360 FPS.
All traces triggered on velocity probe #1.
Record/Reproduce Bandwidth was DC to 32KHz.

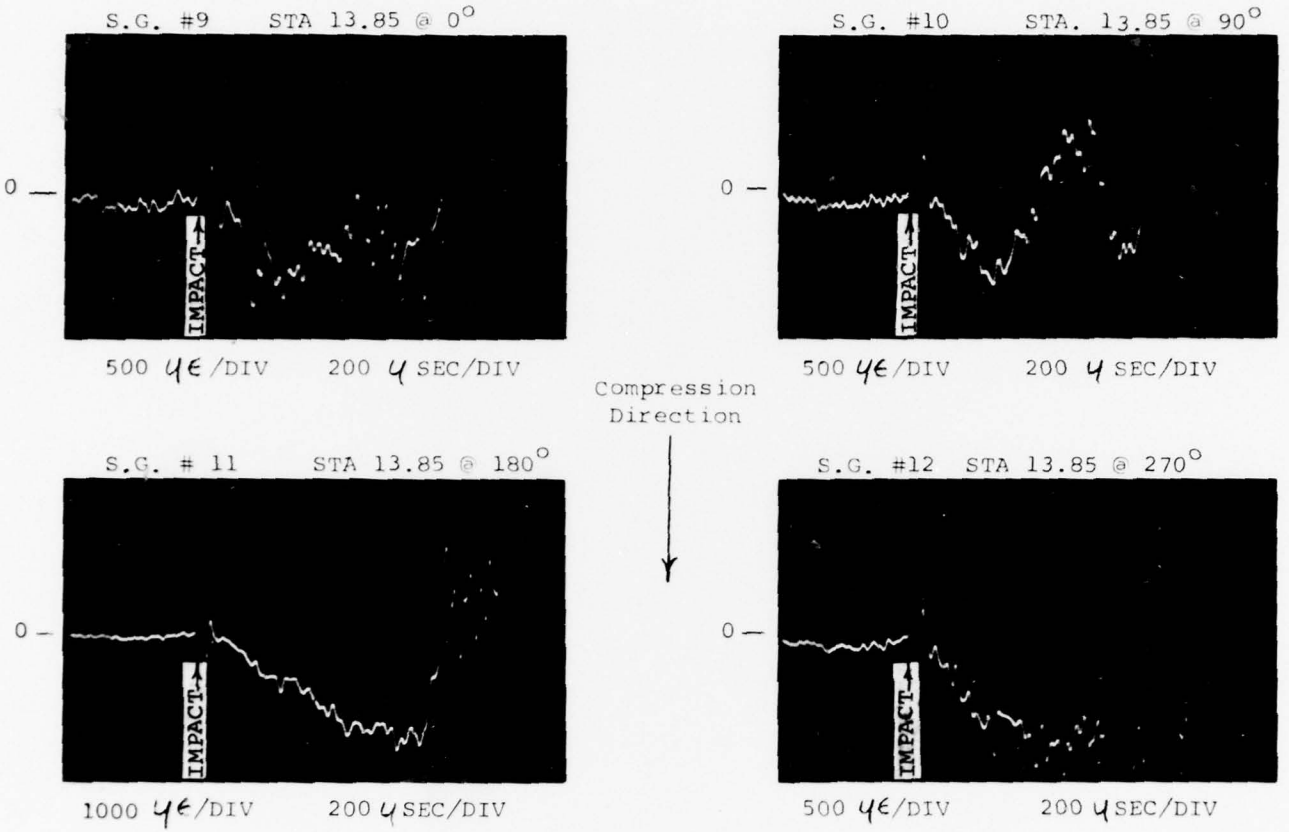

97-344

Figure 29. Shock attenuation Test 1 internal strain.

E.P. Angle of Attack into 20° oblique concrete @ 1300 FPS.
All traces triggered on velocity probe #1.
Record/Reproduce Bandwidth was D.C. to 32KHz.

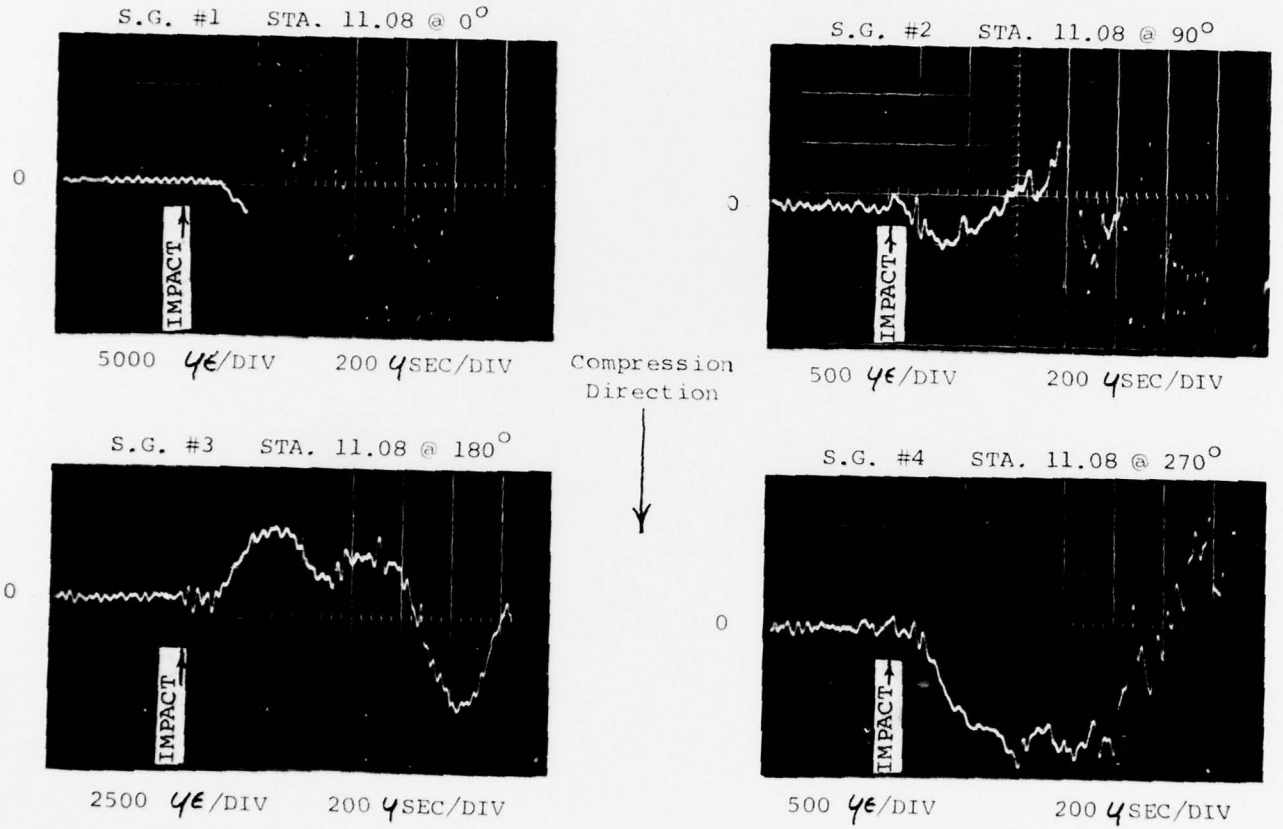

97-345

Figure 30. Shock attenuation Test 2 external strain.

E.P. 0° Angle of Attack into 20° oblique concrete @ 1300 FPS.
All traces triggered on velocity probe #1.
Record/reproduce bandwidth was D.C. to 32KHz.

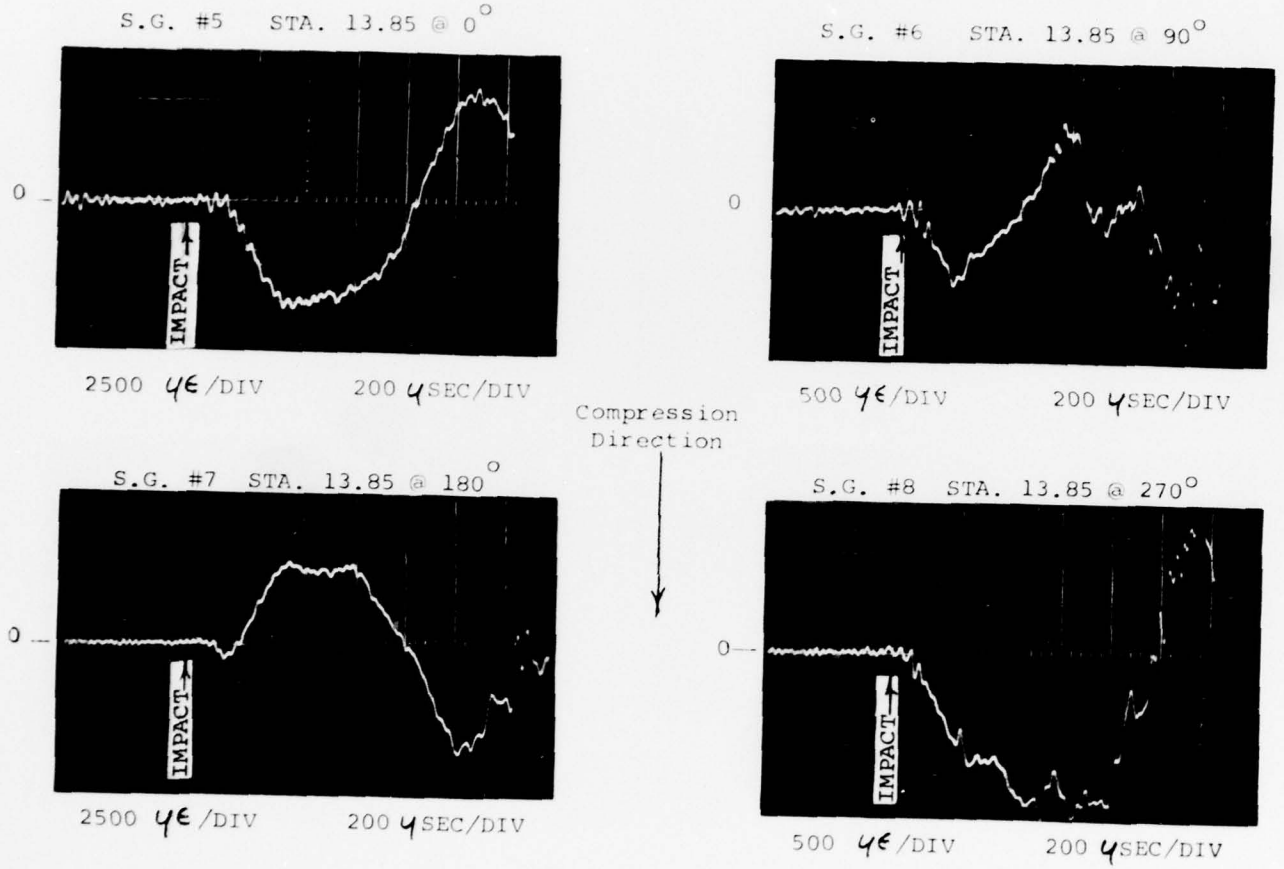

97-346

Figure 31. Shock attenuation Test 2 external strain.

E.P. 0° Angle of attack into 20° oblique concrete @ 1300 FPS.
All traces triggered on velocity probe #1.
Record/reproduce bandwidth was D.C. to 32 KHz.

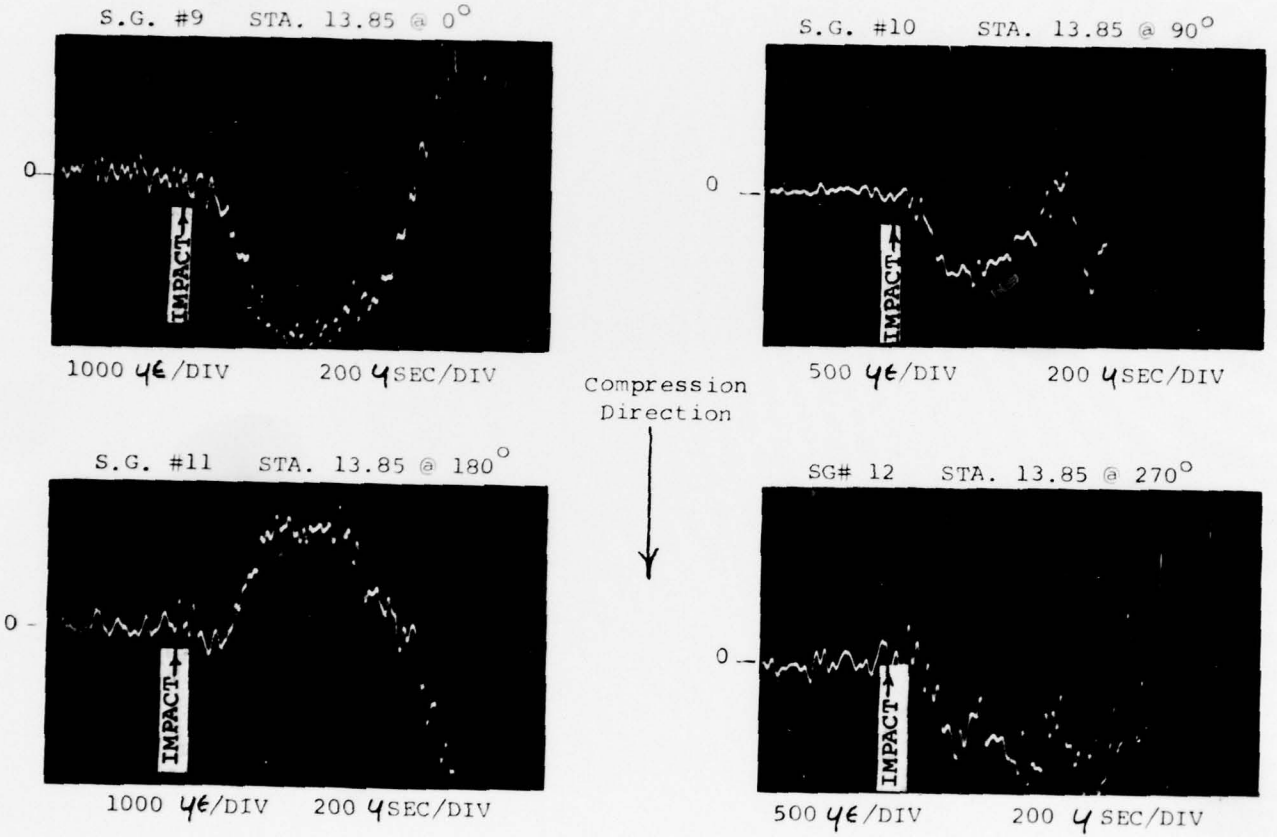

97-347

Figure 32. Shock attenuation Test 2 internal strain.

E. P. @ 5° angle of attack into 0° oblique concrete @ 1050 FPS.
All traces triggered on velocity probe #1. Bandwidth was DC--32KHz.

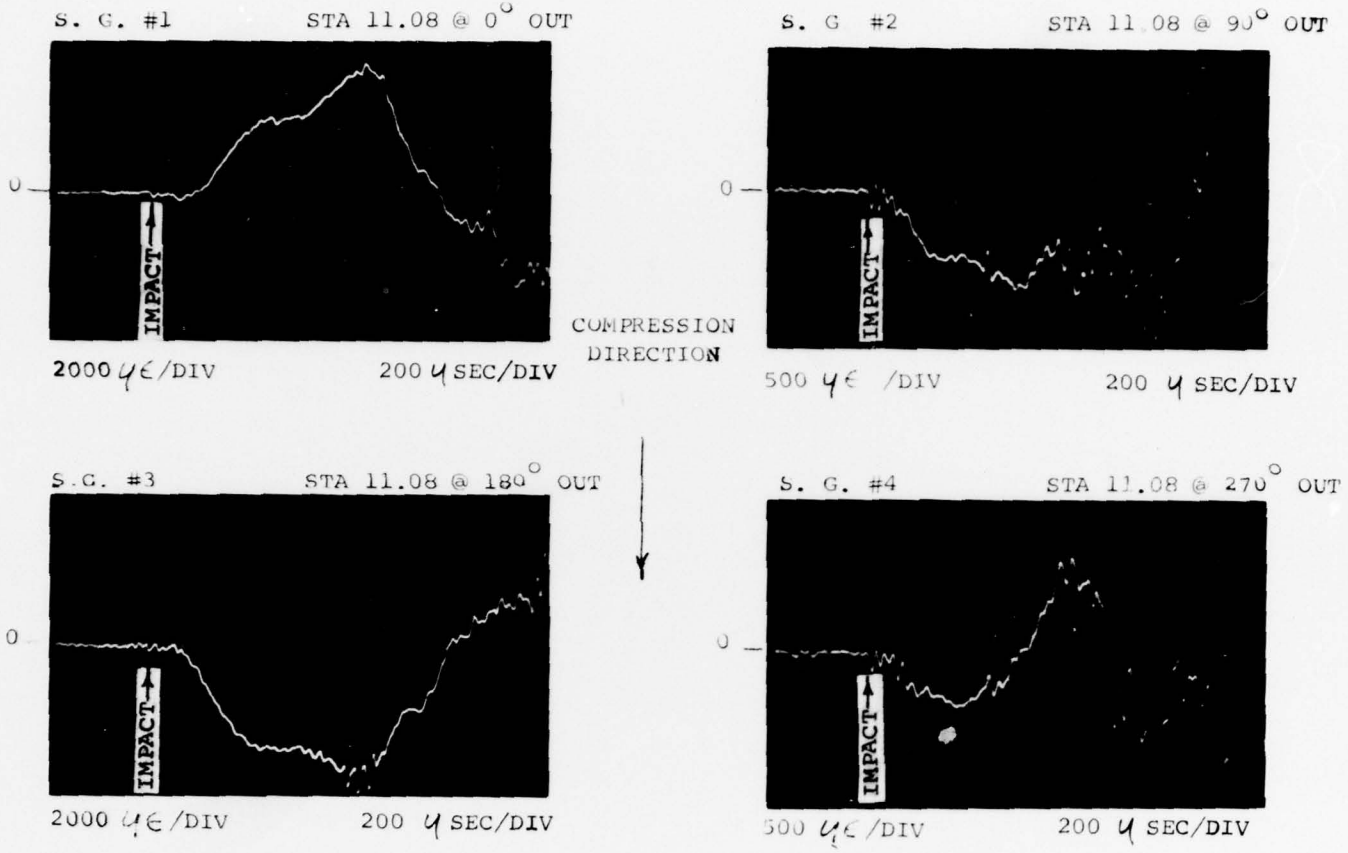

97-348

Figure 33. Shock attenuation Test 3 external strain.

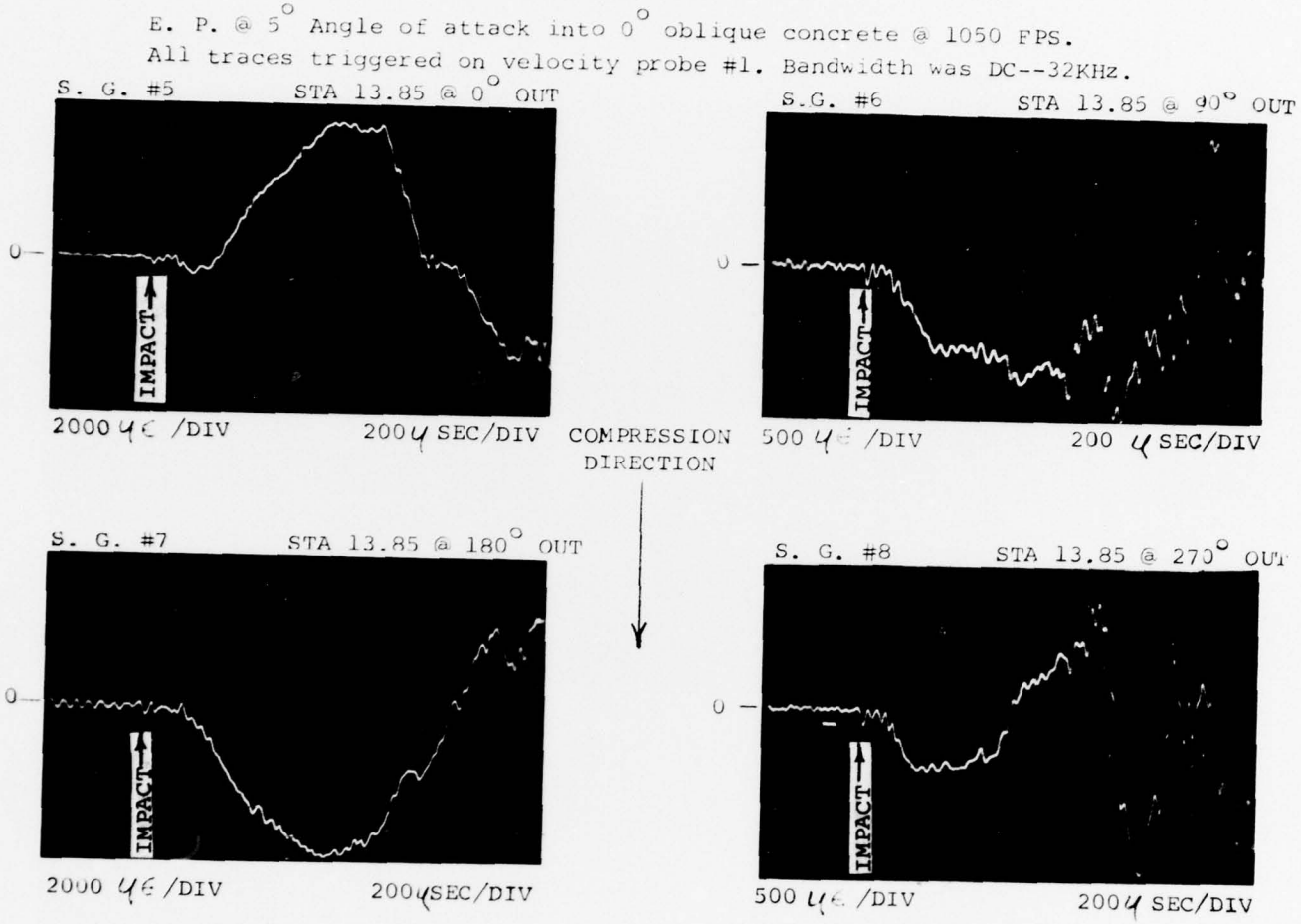

97-349

Figure 34. Shock attenuation Test 3 external strain.

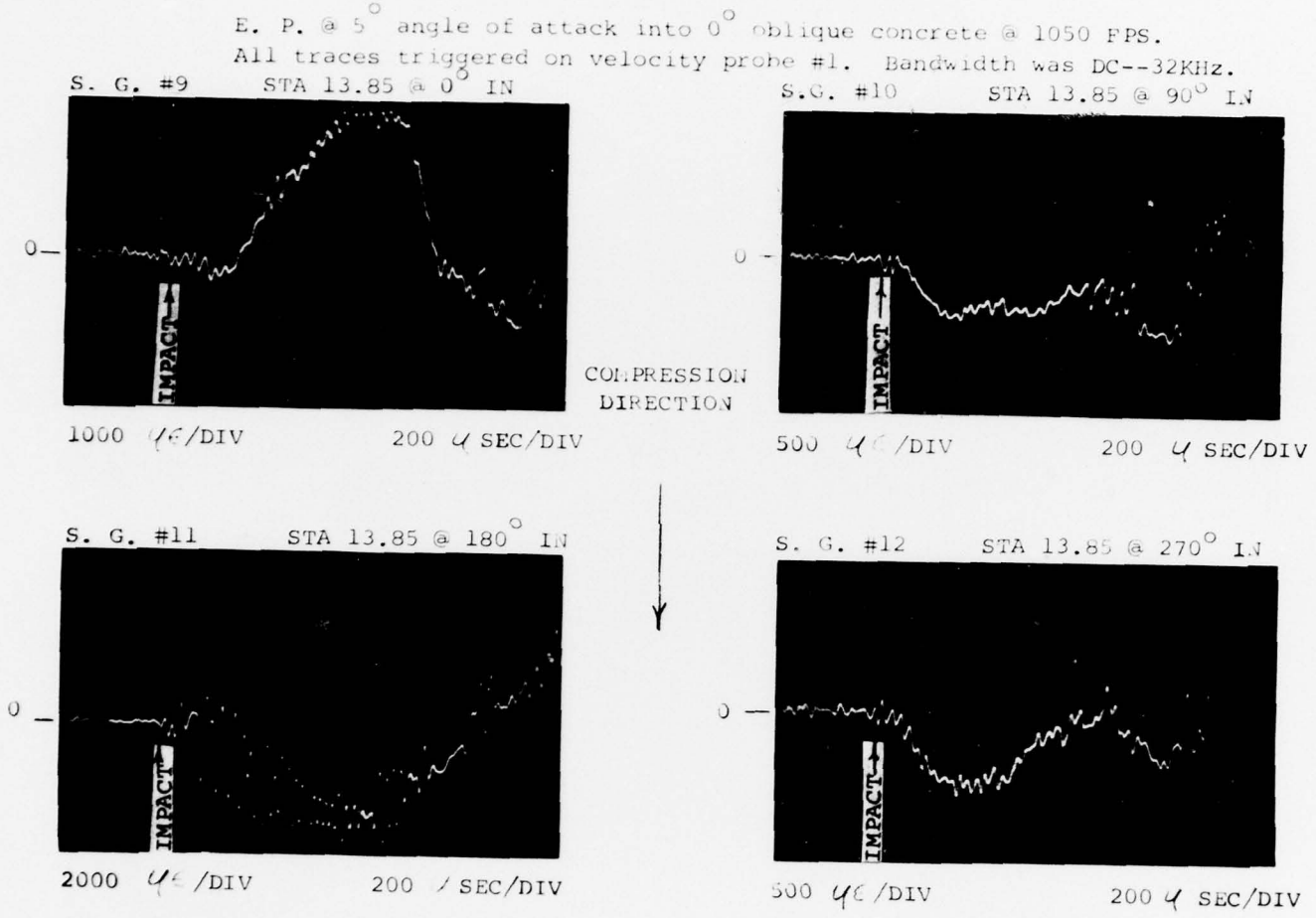

97-350

Figure 35. Shock attenuation Test 3 internal strain.

E. P. @ 5° angle of attack into 0° oblique Glacial Till @ 1750 FPS.
All traces triggered on Impact S. G. #14. Bandwidth was DC--32KHz.

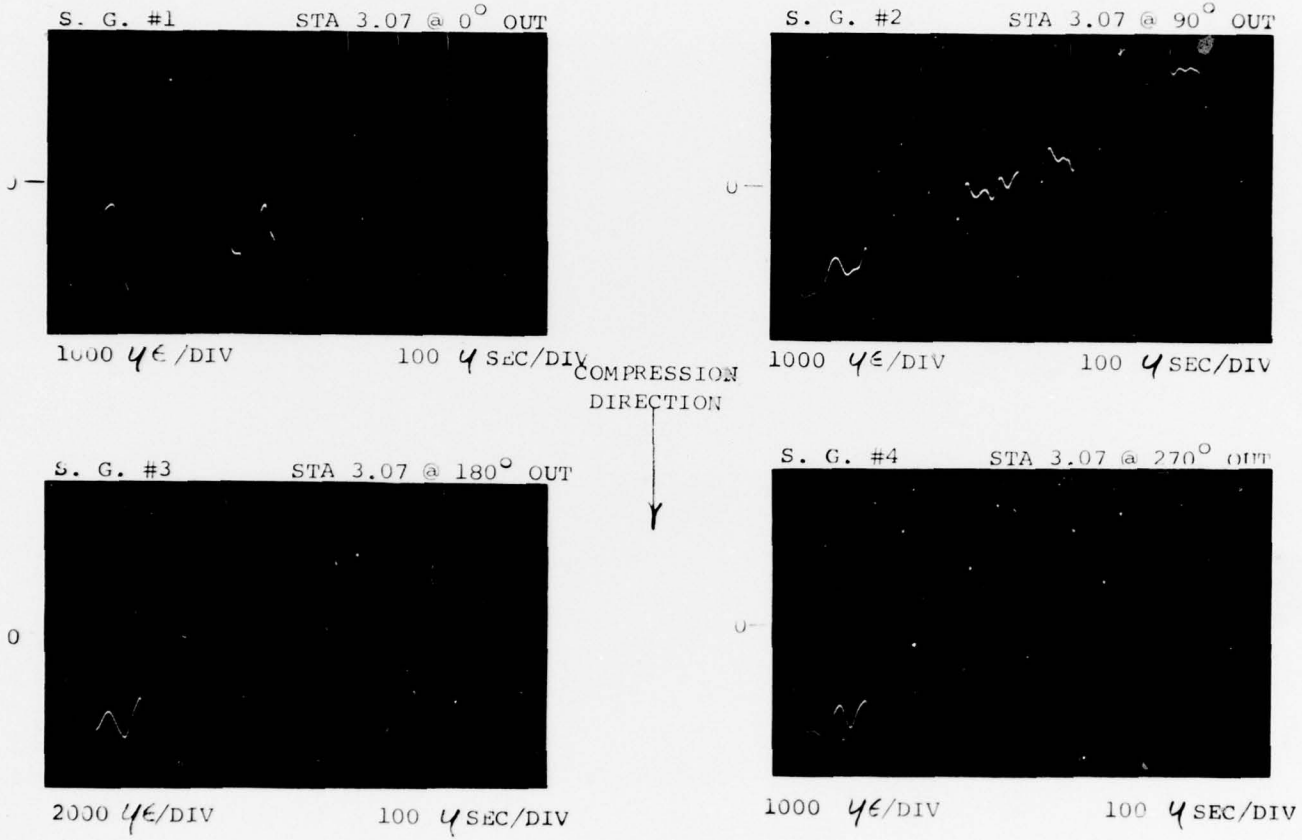

97-351

Figure 36. Shock attenuation Test 4 external strain.

E. P. @ 5° angle of attack into 0° oblique Glacial Till @ 1750 FPS.
All traces triggered on Impact S. G. #14. Bandwidth was DC--32KHz.

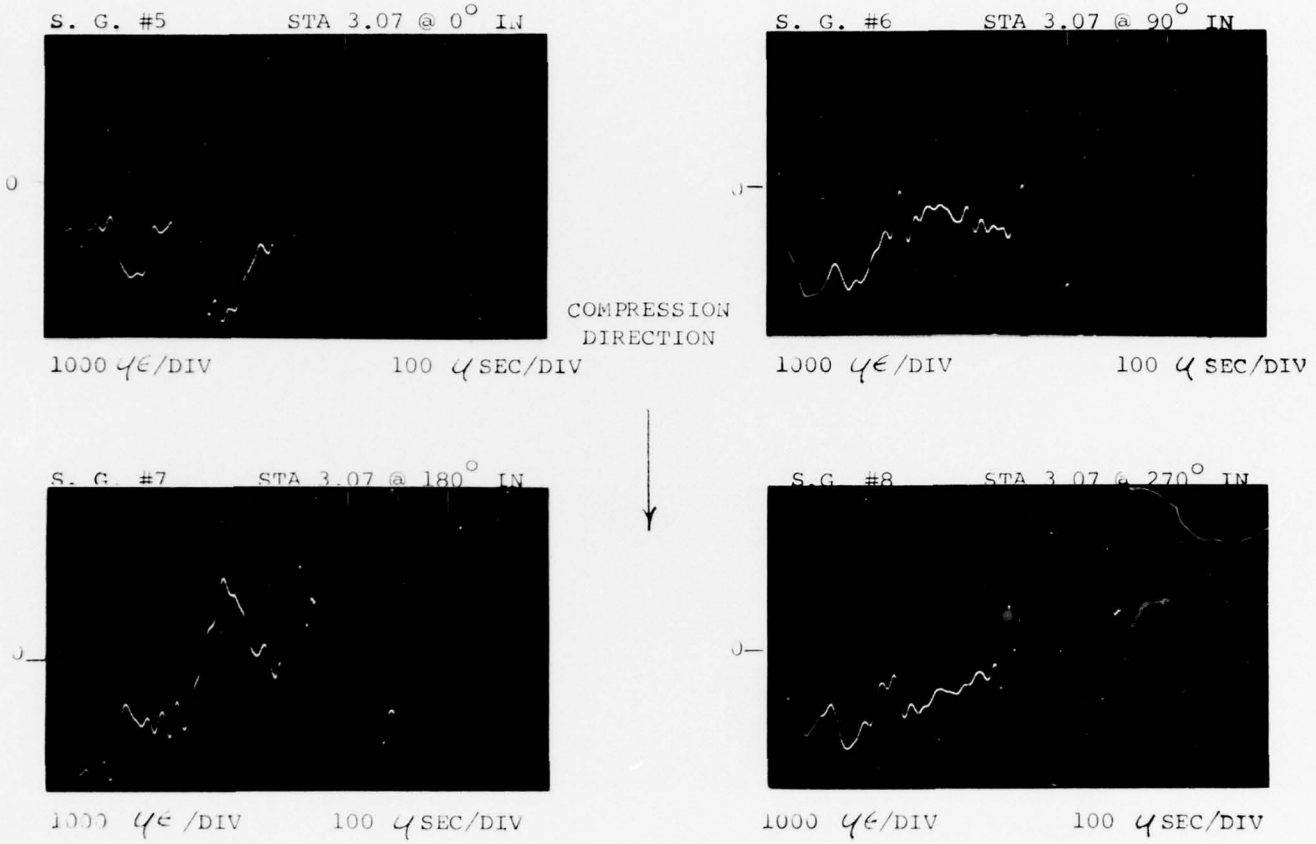

97-352

Figure 37. Shock attenuation Test 4 internal strain.

E. P. @ 5° angle of attack into 0° oblique Glacial Till @ 1750 FPS.
All traces triggered on Impact S. G. #14. Bandwidth was DC--32KHz.

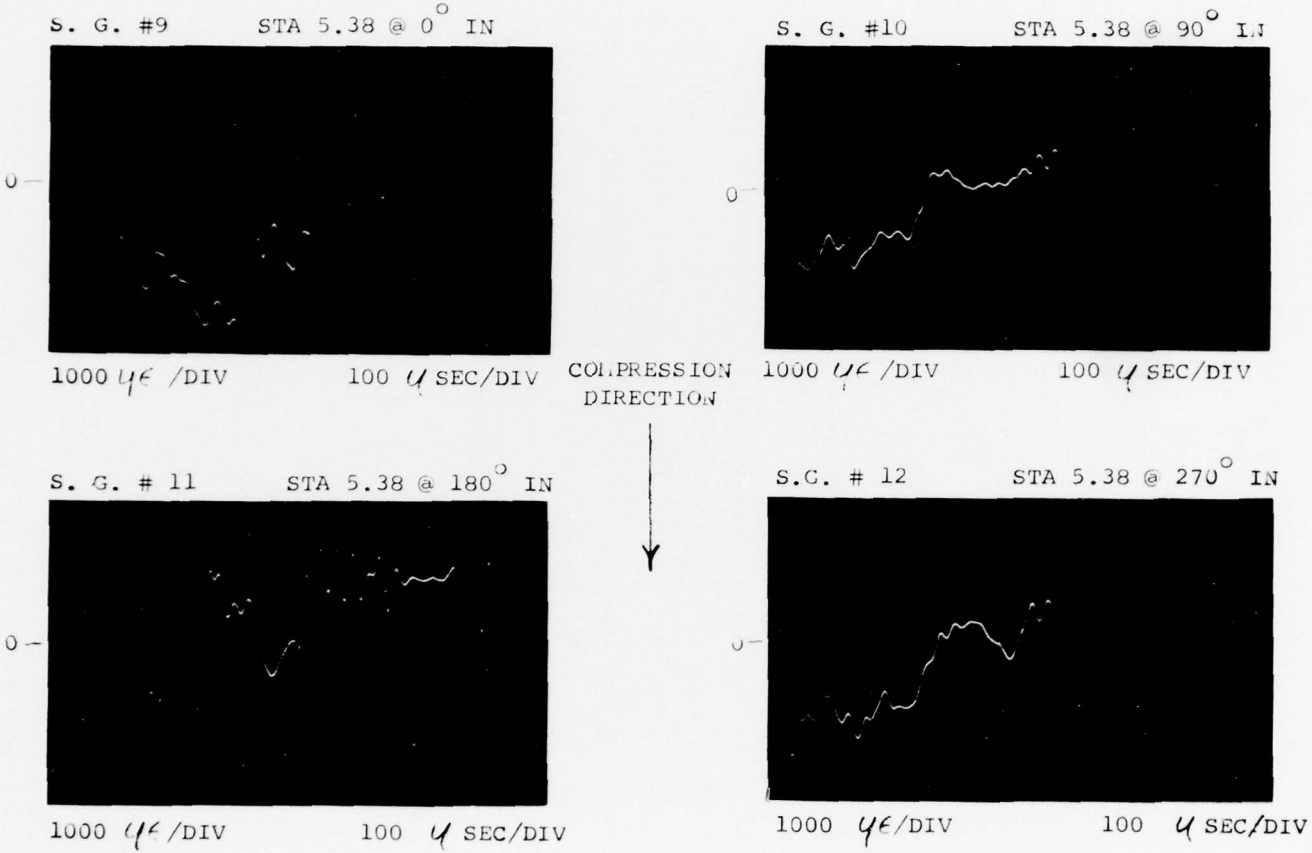

97-353

Figure 38. Shock attenuation Test 4 internal strain.

SECTION VII

CONCLUSIONS

The series of four tests performed on a half-scale and 1/8-scale earth penetrator were successful. Valid acceleration response data was obtained from 9 of the 14 installed accelerometers, however, on some of the data traces, severe ringing (high amplitude, high frequency response at natural frequency of sensor unit or mount) is observed.

The measured impact velocities were less than the desired value of 1500 ft/s for the first three tests and slightly above the desired 1500 ft/s value for the fourth test.

A preliminary examination of the strain response data for Tests 1 and 2 indicates that the concrete media may have cracked or shattered about 300 μsec after impact. This would result in different responses than expected. In addition, the film data for the first two tests did not provide any coverage because of camera timer malfunctioning. For the final two tests the film data indicates that the impacting media remained intact for both tests, the desired EP angle of attack was maintained, and negligible momentum change occurred during the measurement time of interest.

In Tests 1 through 3 a post test inspection of the projectiles indicated no permanent deformation, but in Test 4, the 1/8-scale EP walls collapsed inward. It is believed that the damage occurred during penetration of the 1.5 inch thick aluminum base plate and hence, after the data range of interest.

REFERENCES

1. Henderson, D., Impact and Penetration Technology Program - Parametric Study, Final Report, DNA 3921, dated 7 May 1976.
2. Henderson, D., D. K. Maynard, Impact and Penetration Technology Program - Reverse Ballistic Tests. (Private Communication.)
3. Giara, E. J. and D. K. Maynard, Impact and Penetration Technology Program - P-2 Reverse Ballistic Program, Final Report, Avco document, AVSD-0352-76-CR, dated November 1976.
4. Stephens, R. L., Test Report for 20mm Ballistic Test into Glacial Till, Avco Technical Report K400-T-1586, 5 Feb. 1974.
5. Sandia Drawing No. 517186.

DISTRIBUTION LIST

DEPARTMENT OF DEFENSE

Director
Defense Advanced Rsch. Proj. Agency
ATTN: Tech. Library

Director
Defense Civil Preparedness Agency
ATTN: Admin. Officer

Defense Documentation Center
12 cy ATTN: TC

Director
Defense Intelligence Agency
ATTN: Charles A. Fowler
ATTN: Tech. Library
ATTN: DI-7E
ATTN: DT-2, Wpns. & Sys. Div.
ATTN: DB-4C, Edward O'Farrell

Director
Defense Nuclear Agency
ATTN: SPAS
ATTN: TISI, Archives
ATTN: DDST
3 cy ATTN: TITL, Tech. Library
5 cy ATTN: SPSS

Commander
Field Command, Defense Nuclear Agency
ATTN: FCPR

Director
Interservice Nuclear Weapons School
ATTN: Doc. Control

Director
Joint Strat. Tgt. Planning Staff
ATTN: STINFO, Library

Chief
Livermore Division, Fld. Command, DNA
Lawrence Livermore Laboratory
ATTN: FCPRL

Under Sec'y of Def. for Rsch. & Engrg.
ATTN: S&SS (OS)

DEPARTMENT OF THE ARMY

Dep. Chief of Staff for Rsch. Dev. & Acq.
ATTN: DAMA(CS), MAJ A. Gleim
ATTN: DAMA-CSM-N, LTC G. Ogden
ATTN: Tech. Library

Chief of Engineers
2 cy ATTN: DAEN-MCE-D
2 cy ATTN: DAEN-RDM

Deputy Chief of Staff for Ops. & Plans
ATTN: Dir. of Chem. & Nuc. Ops.
ATTN: Tech. Library

DEPARTMENT OF THE ARMY (Continued)

Chief
Engineer Strategic Studies Group
ATTN: DAEN-FES

Project Manager
Gator Mine Program
ATTN: E. J. Linddsey

Commander
Harry Diamond Laboratories
ATTN: DELHD-NP
ATTN: DRXDO-RBH, James H. Gwaltney

Commander
Picatinny Arsenal
ATTN: Paul Harris
ATTN: Ernie Zimpo
ATTN: P. Angelloti
ATTN: Tech. Library
ATTN: Ray Moesner
ATTN: Marty Margolin
ATTN: Jerry Pental
ATTN: SMUPA-AD-D-A-7
ATTN: SMUPA-AD-D-A
ATTN: SMUPA-AD-D-M
ATTN: B. Shulman, DR-DAR-L-C-FA

Commander
Redstone Scientific Information Ctr.
ATTN: Chief, Documents

Commander
US Army Armament Command
ATTN: Tech. Library

Director
US Army Ballistic Research Labs.
ATTN: J. H. Keefer, DRDAR-BLE
ATTN: J. W. Apgar
ATTN: DRXBR-TB
ATTN: G. Roecker
ATTN: G. Grabarek
ATTN: DRXBR-X
ATTN: A. Ricchiazzi
2 cy ATTN: Tech. Library, Edward Baicy

Commander and Director
US Army Cold Region Res. Engr. Lab.
ATTN: G. Swinzow

Commander
US Army Comb. Arms Combat Dev. Acty.
ATTN: LTC G. Steger
ATTN: LTC Pullen

Commander
US Army Engineer Center
ATTN: ATSEN-SY-L

Division Engineer
US Army Engineer Div., Huntsville
ATTN: HNDED-SR

DEPARTMENT OF THE ARMY (Continued)

Division Engineer
US Army Engineer Div., Missouri Rvr.
ATTN: Tech. Library

Commandant
US Army Engineer School
ATTN: ATSE-TEA-AD
ATTN: ATSE-CTD-CS

Director
US Army Engr. Waterways Exper. Sta.
ATTN: William Flathau
ATTN: Guy Jackson
ATTN: D. K. Butler
ATTN: Tech. Library
ATTN: John N. Strange
ATTN: P. Hadala
ATTN: Leo Ingram
ATTN: Behzad Rohani

Commander
US Army Mat. & Mechanics Rsch. Ctr.
ATTN: Tech. Library

Commander
US Army Materiel Dev. & Readiness Cmd.
ATTN: Tech. Library

Director
US Army Materiel Sys. Analysis Acty.
ATTN: Joseph Sperazza

Commander
US Army Missile Command
ATTN: F. Fleming
ATTN: W. Jann
ATTN: J. Hogan

Commander
US Army Mobility Equip. R&D Ctr.
ATTN: STSFB-MW
ATTN: Tech. Library
ATTN: STSFB-XS

Commander
US Army Nuclear Agency
ATTN: Tech. Library
ATTN: Doc. Control

Commander
US Army Training and Doctrine Comd.
ATTN: LTC Auveduti, COL Enger
ATTN: LTC J. Foss

Commandant
US Army War College
ATTN: Library

US Army Mat. Cmd. Proj. Mngr. for Nuc. Munitions
ATTN: DRCPM-NUC

DEPARTMENT OF THE NAVY

Chief of Naval Operations
ATTN: OP 982, CAPT Toole
ATTN: Code 604C3, Robert Piacesi
ATTN: OP 982, LCDR Smith
ATTN: OP 982, LTC Dubac

DEPARTMENT OF THE NAVY (Continued)

Chief of Naval Research
ATTN: Tech. Library

Officer-in-Charge
Civil Engineering Laboratory
ATTN: R. J. Odello
ATTN: Tech. Library

Commandant of the Marine Corps
ATTN: POM

Commanding General
Development Center, Fire Support Branch
ATTN: CAPT Hartneady
ATTN: LTC Gapenski

Commander
Naval Air Systems Command
ATTN: F. Marquardt

Commanding Officer
Naval Explosive Ord., Disposal Fac.
ATTN: Code 504, Jim Petrousky

Commander
Naval Facilities Engineering Command
ATTN: Tech. Library

Superintendent (Code 1424)
Naval Postgraduate School
ATTN: Code 2124, Tech. Rpts. Librarian

Director
Naval Research Laboratory
ATTN: Code 2600, Tech. Library

Commander
Naval Sea Systems Command
ATTN: SEA-9931G
ATTN: ORD-033

Officer-in-Charge
Naval Surface Weapons Center
ATTN: M. Kleinerman
ATTN: Code WX21, Tech. Library
ATTN: Code WA501, Navy Nuc. Prgms. Off.

Commander
Naval Surface Weapons Center
ATTN: Tech. Library

Commander
Naval Weapons Center
ATTN: Carl Austin
ATTN: Code 533, Tech. Library

Commanding Officer
Naval Weapons Evaluation Facility
ATTN: Tech. Library

Director
Strategic Systems Project Office
ATTN: NSP-43, Tech. Library

DEPARTMENT OF THE AIR FORCE

AF Armament Laboratory, AFSC
ATTN: Masey Valentine
3 cy ATTN: John Collins, AFATL/DLYV

DEPARTMENT OF THE AIR FORCE (Continued)

AF Institute of Technology, AU
ATTN: Library, AFIT, Bldg. 640, Area B

AF Weapons Laboratory, AFSC
ATTN: SUL

Assistant Sec'y of the Air Force
Research and Development
ATTN: Col R. E. Steere

Deputy Chief of Staff
Research and Development
ATTN: Col J. L. Gilbert

Commander, Foreign Technology Division, AFSC
ATTN: NICD, Library

HQ USAF/IN
ATTN: INATA

HQ USAF/RD
ATTN: RDPM

Oklahoma State University
Fld. Off. for Wpns. Effectiveness
ATTN: Edward Jackett

Commander, Rome Air Development Center, AFSC
ATTN: EMTLD, Doc. Library

SAMSO/RS
ATTN: RSS

DEPARTMENT OF ENERGY

Albuquerque Operations Office
ATTN: Doc. Con. for Tech. Library

Division of Headquarters Services
ATTN: Doc. Con. for Class Tech. Library

Nevada Operations Office
ATTN: Doc. Con. for Tech. Library

Division of Military Application
ATTN: Doc. Control for Test Office

University of California
Lawrence Livermore Laboratory
ATTN: Tech. Info. Dept., L-3
ATTN: Jerry Goudreau
ATTN: Mark Wilkins, L-504

Los Alamos Scientific Laboratory
ATTN: Doc. Control for Tom Dowler
ATTN: Doc. Control for Reports Lib.

Sandia Laboratories, Livermore Laboratory
ATTN: Doc. Control for Tech. Library

Sandia Laboratories
ATTN: Doc. Con. for John Keizur
ATTN: Doc. Con. for William Caudle
ATTN: Doc. Con. for 3141, Sandia Rpt. Coll.
ATTN: Doc. Con. for John Colp
ATTN: Doc. Con. for W. Altsmeirer
ATTN: Doc. Con. for Walter Herrmann
ATTN: Doc. Con. for William Patterson

OTHER GOVERNMENT AGENCIES

NASA
Ames Research Center
ATTN: Robert W. Jackson

Office of Nuclear Reactor Regulation
Nuclear Regulatory Commission
ATTN: Robert Heineman
ATTN: Lawrence Shao

DEPARTMENT OF DEFENSE CONTRACTORS

Aerospace Corporation
ATTN: Tech. Info. Services

Agbabian Associates
ATTN: M. Agbabian

Applied Theory, Inc.
2 cy ATTN: John G. Trulio

Avco Research & Systems Group
ATTN: Research Lib., A830, Rm. 7201
ATTN: David Henderson
ATTN: Pat Grady
ATTN: S. Skemp, J200
ATTN: E. J. Giara, Jr.

Battelle Memorial Institute
ATTN: Tech. Library

The BDM Corporation
ATTN: Tech. Library

The Boeing Company
ATTN: Aerospace Library

California Research & Technology, Inc.
ATTN: Ken Kreyenhagen
ATTN: Tech. Library

Civil/Nuclear Systems, Corp.
ATTN: Robert Crawford

EG&G, Inc., Albuquerque Division
ATTN: Tech. Library

Engineering Societies Library
ATTN: Ann Mott

General Dynamics, Corp.
Pomona Division
ATTN: Keith Anderson

General Electric Company
TEMPO-Center for Advanced Studies
ATTN: DASIAC

Georgia Institute of Technology
ATTN: L. W. Rehfield
ATTN: S. V. Hanagud

Honeywell, Inc.
Defense Systems Division
ATTN: T. N. Helvig

Institute for Defense Analyses
ATTN: IDA, Librarian, Ruth S. Smith

DEPARTMENT OF DEFENSE CONTRACTORS (Continued)

Kaman AviDyne
Division of Kaman Sciences Corp.
ATTN: E. S. Criscione
ATTN: Norman P. Hobbs
ATTN: Tech. Library

Kaman Sciences Corporation
ATTN: Library

Lockheed Missiles & Space Co., Inc.
ATTN: M. Culp
ATTN: Tech. Library

Lockheed Missiles and Space Co., Inc.
ATTN: Tech. Info. Ctr., D/Coll.

Martin Marietta Corporation
Orlando Division
ATTN: Al Cowen
ATTN: H. McQuaig
ATTN: M. Anthony

Merritt CASES, Inc.
ATTN: Tech. Library
ATTN: J. L. Merritt

University of New Mexico
Dept. of Campus Security and Police
ATTN: G. E. Triandafalidis

Nathan M. Newmark
Consulting Engineering Services
ATTN: Nathan M. Newmark
ATTN: W. Hall

Pacifica Technology
ATTN: R. Bjork
ATTN: G. Kent

Physics International Company
ATTN: Doc. Con. for Tech. Library
ATTN: Doc. Con. for Larry A. Behrmann
ATTN: Doc. Con. for Dennis Orphal

DEPARTMENT OF DEFENSE CONTRACTORS (Continued)

R & D Associates
ATTN: J. G. Lewis
ATTN: Paul Rausch
ATTN: Tech. Library
ATTN: Arlen Fields
ATTN: Cyrus P. Knowles
ATTN: William B. Wright, Jr.
ATTN: Henry Cooper
ATTN: Harold L. Brode

The Rand Corporation
ATTN: Tech. Library

Science Applications, Inc.
ATTN: Tech. Library

SRI International
ATTN: Jim Colton
ATTN: George R. Abrahamson

Systems, Science and Software, Inc.
ATTN: Edward Gaffney
ATTN: Robert Sedgewick
ATTN: Tech. Library

Terra Tek, Inc.
ATTN: Tech. Library

TRW Defense & Space Sys. Group
ATTN: Tech. Info. Center/S-1930
ATTN: Peter K. Dai, R1/2170

TRW Defense & Space Sys. Group
San Bernardino Operations
ATTN: E. Y. Wong, 527/712

Weidlinger Assoc. Consulting Engineers
ATTN: J. M. McCormick
ATTN: Melvin L. Baron

Weidlinger Assoc. Consulting Engineers
ATTN: J. Isenberg